ELSEVIER

Chemical Geology 240 (2007) 61–84

CHEMICAL GEOLOGY
INCLUDING
ISOTOPE GEOSCIENCE

www.elsevier.com/locate/chemgeo

Complex proterozoic to paleozoic history of the upper mantle recorded in the Urals lherzolite massifs by Re–Os and Sm–Nd systematics

Svetlana G. Tessalina [a,*], Bernard Bourdon [a,1], Abdelmouhcine Gannoun [a,b], Françoise Capmas [a], Jean-Louis Birck [a], Claude J. Allègre [a]

[a] *Laboratoire de Géochimie et Cosmochimie, IPGP, T 14-24, 4 place Jussieu, 75252 Paris Cedex 05, France*
[b] *Department of Earth Sciences, The Open University, Walton Hall, Milton Keynes MK7 6AA, UK*

Received 16 September 2005; received in revised form 16 January 2007; accepted 3 February 2007

Editor: S.L. Goldstein

Abstract

Re–Os and Sm–Nd isotope systematics for the Nurali and the Mindyak lherzolite massifs have been determined in conjunction with their whole-rock major and trace element contents. The data suggest that the peridotites represent residues after the extraction of up to 25% of partial melt from the fertile mantle protolith. Later melt percolation and associated fluid-rock reaction events have modified the Sm/Nd, Re/Os and Pd/Os ratios of peridotites, but didn't affect significantly their major element compositions.

The Re–Os and Sm–Nd isotope data strongly suggest that several magmatic events are involved in the evolution of these bodies. The mantle sections of these complexes formed during Proterozoic times, represent the first reported evidence for Precambrian peridotites in the Southern Urals.

The oldest Re–Os age of 1250±80 Ma for the Nurali cumulates records the separation from the convective upper mantle. Multiple partial melting of the peridotites followed by fractional crystallisation produced layered cumulates which were subsequently stored in the sub-continental lithosphere over ~0.8 Ga. The age of the Nurali ophiolite coincides with the development of an epicontinental rift basin on the passive margin of the Baltica proto-continent.

The younger Sm–Nd age of Mindyak peridotites (882±83 Ma) and Re–Os age of associated gabbros (804±37 Ma) record another tectonic event responsible for the separation of the Mindyak massif from convective mantle. Between ~850 and 650 Ma, the margins of the paleo-Asian ocean became the site of island-arc formation. This ophiolite then evolved in an intra-oceanic island-arc setting. The Mindyak lherzolite massif could be the first record of a Neoproterozoic Cadomian arc in the Southern Urals.

A later island-arc formation event has then affected both massifs in different ways. The Mindyak massif was incorporated into a rifting zone at ~ 500 Ma, producing a second partial melting event of peridotites, cross-cutted by mafic dykes. The Nurali massif has also been cross-cut by gabbro-diorite dykes at Devonian time during the subduction event leading to Urals island-arc formation.

* Corresponding author.
E-mail address: svetes@ipgp.jussieu.fr (S.G. Tessalina).
[1] Now at: Institute of Isotope Geochemistry and Mineral Resources, Department of Earth Sciences, ETH Zürich, CH-8092 Zürich, Switzerland.

0009-2541/$ - see front matter
doi:10.1016/j.chemgeo.2007.02.006

The combination of ^{187}Re–^{187}Os and ^{147}Sm–^{143}Nd systematics for peridotites, mafic–ultramafic cumulates and mafic dykes reveals the complex history of ophiolite complexes, including isolation from the convective upper mantle at Proterozoic time, storage in sub-continental lithospheric mantle and re-activation during later tectonic events, such as island-arc formation.

Keywords: Ophiolites; Orogenic lherzolite massif; Re–Os isotope systematics; Urals

1. Introduction

Orogenic lherzolite massifs are portions of the upper mantle emplaced in the upper crust during major tectonic events. These massifs usually outcrop along major fault zones, where the interaction between oceanic and crustal materials takes place. Studies of trace elements and Sr–Nd–Pb–Os isotope systematics in lherzolite massifs around the world have provided useful information about the evolution, composition and structure of the upper mantle (Loubet and Allègre, 1982; Reisberg et al., 1991; Pearson et al., 1993; Brueckner et al., 1995; Roy-Barman et al., 1996; Meisel et al., 1996; Pearson et al., 2004). In particular, it has been shown that lherzolite massifs have undergone a complex evolution including successive partial melting events with subsequent differentiation of the melts. Such events are likely to have occurred within the upper mantle and therefore may reflect the multi-stage history of mantle material (Loubet and Allègre, 1982).

Combined Re–Os and Sm–Nd isotope systematics of Beni-Bousera (Morocco), Baldissero and Lanzo, Italian Alps, and Lherz massifs, France (Roy-Barman et al., 1996); Ronda massif (Spain) (Reisberg et al., 1991); various Swiss Alps massifs (Meisel et al., 1996); Zabargad (Red Sea) (Brueckner et al., 1995) have shown the existence of small scale mantle heterogeneities (e.g., Roy-Barman et al., 1996); highly depleted Os isotope compositions and old Proterozoic model ages for these massifs (e.g., Meisel et al., 1996) and the incorporation of peridotites (Meisel et al., 1996) or cumulates (Roy-Barman et al., 1996) into the sub-continental lithospheric mantle 1 or 2 Ga ago (Reisberg et al., 1991; Reisberg and Lorand, 1995).

There is a heated debate concerning the formation age, geological setting and history of emplacement of lherzolite complexes in the Southern Urals. They have been interpreted as an ophiolite sequence characterized by weakly depleted oceanic mantle and thought to have originated in rift basins of the East European continental margin (Savelieva et al., 1997, 2002) or in a mid-ocean ridge setting (Kamaletdinov and Kazantseva, 1983). They have also been considered as pieces of sub-continental lithospheric mantle (SCLM) that have been exhumed at a continent–ocean transition zone (Garuti et al., 1997; Zaccarini et al., 2002). New constraints on the origin of the ultramafic lherzolites based on combined Re–Os and Sm–Nd data may go some way to addressing this controversy. The Re–Os isotope system has been largely used for the study of mafic–ultramafic complexes because of its unique properties (e.g., Reisberg and Lorand, 1995). The large fractionation between Re and Os during mantle melting makes this isotope system extremely useful for dating fractionation associated with magmatic processes. Furthermore, the Re–Os system, combined with Sr, Nd and Pb (Ellam et al., 1992) is an ideal tracer of sub-lithospheric source materials. Unlike Re and Os which are typically siderophile and chalcophile, Sm and Nd are lithophile elements that are enriched in the continental crust relative to the mantle. As Sm/Nd ratios are fractionated between the depleted MORB mantle (DMM) and the continental crust, these two reservoirs have developed very distinct isotope signatures through time. Thus, any contribution of Nd from an old continental crust to a mantle-derived rock or melt can be easily detected.

This study focuses on three issues: (1) the age relationship of the ultramafic rocks and mafic intrusions within the lherzolite–harzburgite complexes in the Southern Urals; (2) the geodynamic setting (rifting or subduction); and (3) the origin of the mantle section (sub-continental lithospheric mantle or oceanic).

2. Geological setting and structure

The Urals is one of the best preserved Late Paleozoic arc–continent collision zone developed by subduction and collision between the Eastern European Craton to the west and the Magnitogorsk island-arc to the east (Puchkov, 1997; Brown et al., 1998). The Urals mafic–ultramafic complexes have been subdivided into three main types: (1) lherzolite–harzburgite complexes; (2) harzburgite–dunite–volcanics ophiolite complexes in the Southern Urals; and (3) zoned dunite–clinopyroxenite–gabbro complexes (Urals–Alaskan type) in the

Middle Urals Platinum belt (Savelieva et al., 2002). The lherzolite massifs occur in an allochtonous position thrusting onto the East European Craton, or as blocks within the Main Urals fault considered to represent the suture zone of the orogen (Nurali and Mindyak) (Fig. 1 A). The Nurali and Mindyak lherzolite complexes are located in a mélange zone of the Main Urals Fault near the town of Miass (South Urals) (Fig. 1 B). They form east-dipping (70–80°) lens-shaped bodies overlying either crystalline schists of the Eastern European craton or its Paleozoic sedimentary cover. To the east, the mélange zone comprises Late Ordovician cherty sediments and basalts, Silurian–Devonian volcanics including basalts, andesites and rhyodacites, epiclastic rocks, and carbonate sediments (Savelieva et al., 1997).

The Mindyak and Nurali massifs consist of mantle units characterised by fertile peridotites with upwardly decreasing pyroxene contents and dunite-rich zones at the top of each. The lherzolite is coarse-grained, with porphyroclastic textures and consists of olivine (50–60 modal%), enstatite and diopside. A harzburgite unit overlies the lherzolite and consists of olivine (80–85% in volume), enstatite, Cr-spinel and minor diopside. Dunite is interlayered within the harzburgite. This mantle unit is overlaid by the Moho transition zone (TZ) represented by a layered sequence of dunite, wehrlite, clinopyroxenite, websterite and chromitites (Garuti et al., 1997). Wehrlite and clinopyroxenite cumulates form 2–8 cm-thick olivine-rich and clinopyroxene-rich layers and lenses within a 200 m thick transition zone (Pertsev et al., 1997). The layered Nurali transition zone shows the typical order of layered gabbros in ophiolites. This TZ has been interpreted as a result of a multistage crystallisation in shallow magma chambers within a rift zone (Pertsev et al., 1997). Garnet-bearing websterite and pyroxenite occur in Mindyak, suggesting that the massif might have undergone high-pressure equilibration at some stage of its evolution (Garuti et al., 1997). Within the Nurali massif, gabbro and oxide-bearing diorite lie between the transition zone and the mélange zone. On the basis of field relationships (gabbro apophyses within TZ, ultramafic xenoliths in the gabbro), Pertsev et al. (1997) suggest that the gabbros intrude the layered cumulates. There are no dyke units or pillow-lavas within the Nurali and Mindyak sequence; these units were either originally lacking, or structurally removed by subsequent tectonic activity and now occur as exotic blocks in adjacent serpentinite mélange zones.

Twenty-eight mafic and ultramafic samples were selected to span the entire compositional range of the massifs. Ten plagioclase- and spinel-bearing lherzolite, harzburgite and dunite samples represent mantle units from Mindyak and Nurali massifs. Eight wehrlite and clinopyroxenite cumulate samples were chosen from the transition zone. A chromitite sample was found within an altered orthopyroxenite xenolith in the ultramafic cumulates of the Nurali massif, and the seven amphibole-bearing gabbro and diorite samples were from structural units above these layered ultramafic cumulates. Gabbro dyke samples (My 28 and My 32) are from the mantle unit within the Mindyak massif. All these samples have been previously analysed for platinum group elements, Ni, Au and Cu contents (Garuti et al., 1997).

3. Previous geochronological studies

The formation of oceanic crust in Urals ophiolites has been dated as Early Devonian to Middle Ordovician (about 390 Ma to 470 Ma) by Sm–Nd mineral and whole-rock isochrons on ultramafics and gabbros from the Kempersai massif (Edwards and Wasserburg, 1985; Melcher et al., 1999) and by K/Ar whole-rock and mineral ages from the Khabarny (Southern Urals) complex (Pushkarev and Kaleganov, 1993), and the Voikar–Syninsky (Polar Urals) complexes (Knipper and Perfiliev, 1979). There is little data for lherzolite–harzburgite complexes. Within the Mindyak massif, only garnet metagabbros blocks from a serpentinite tectonic breccia adjacent to the mantle and TZ sequence were used for geochronological studies. The published U–Pb, Pb–Pb and Sm–Nd isotope data define an age of 410–415 Ma, which corresponds to the peak of a metamorphic event in this area (Scarrow et al., 1999). A minimum age of 467 Ma was reported for zircon cores in these rocks and this is interpreted as the gabbro crystallisation age. The U–Pb isochron age for zircons from gabbro-diorite and diorite dykes of the Nurali complex is of 399 Ma (Fershtater et al., 2000), and this has been interpreted as the age of a second intrusive phase (Savelieva et al., 1997).

Re–Os systematics have already been used to date chromites and PGE phases from a number of Urals mafic–ultramafic complexes such as Nijni Tagil, Sissert', Kempersai and Ray-Iz (Luck and Allègre, 1991; Hattori and Hart, 1991; Walker et al., 2002). Almost all the samples have a limited range in their calculated initial $^{187}Os/^{188}Os$ ratios and they are similar to or greater than the chondritic reference, ranging from 0.12387 ($\gamma_{Os}=-0.36$), for the Kempersai massif up to 0.12707 ($\gamma_{Os}=2.60$) for the Ray Iz ophiolite in the Polar Urals (γ_{Os} is expressed as a percentage difference between the Os isotopic composition of a sample and

the average chondritic composition for a specified time). In only one sample from the northern part of the Kempersai massif (Al-rich chromite), is the initial $^{187}Os/^{188}Os$ ratio of 0.11879 ($\gamma_{Os}=-4.44$) sufficiently low to be considered as ancient, melt-depleted sub-continental lithospheric mantle (Walker et al., 2002).

4. Analytical methods

Whole-rock samples powder was spiked with a mixed ^{149}Sm–^{150}Nd tracer and dissolved using a 1:1 HF+HNO_3 mixture in a Teflon beaker. After evaporation, residues were dissolved in a mixture of 0.9 M boric and nitric acids. Separation of REE from the rock matrix was performed using the TRU-Spec chromatographic columns. Nd and Sm were isolated from the others REEs using HDEHP LN-Spec extraction columns. The Sm and Nd residues were dissolved in 3% HNO_3 acid prior to the isotopic analyses carried out on a Neptune™ multi-collector inductively coupled mass spectrometer (MC-ICP-MS) at the Institut de Physique du Globe in Paris (IPGP). The duration of an analysis is 25 min. The mean value of about 200 single measurements (10 blocks of 20 cycles) was used. The Nd Johnson and Matthey standard yielded $^{143}Nd/^{144}Nd=0.511457\pm20$ ($n=7$, 2σ standard deviation) during the period of measurements; this corresponds to a value of 0.511840 ± 20 for the international Nd standard La Jolla. The Nd isotopic ratios were normalised to $^{146}Nd/^{144}Nd=0.7219$ using an exponential law and the total procedural blank was less then 5 pg for Nd.

Re and Os concentrations and the Os isotopic composition were determined by negative thermal ionisation mass spectrometry (N-TIMS) on a Finnigan MAT 262 at IPGP, as described in Birck et al. (1997). The IPGP Merck Os standard yielded $^{187}Os/^{188}Os=0.1746\pm8$ ($n=4$, 2σ standard deviation) during the period of the measurements and the total procedural blank for Os was 0.040 ± 0.015 pg ($n=7$). The $^{187}Os/^{188}Os$ ratios for the blanks ranged between 0.138 and 0.475 with a mean value of 0.279. The Re blanks ranged between 8 and 10 pg. The samples were prepared for Re–Os analysis using low temperature acid digestion technique. This method was developed by Birck et al. (1997) in order to achieve extremely low procedural blanks at a few tens of parts per trillion (ppt, 10^{-12} g/g) levels for processing low abundance silicate-bearing samples.

Approximately 0.2 g of ultramafic rocks and 0.5 g of mafic rocks samples powder was spiked with a mixed ^{190}Os–^{185}Re spike and then dissolved with HBr and HF in a Teflon bomb at 145 °C. After evaporation, Os was oxidized to OsO_4 in a nitric acid solution containing chromium trioxide in order to ensure spike/sample equilibration. Finally, Os was extracted in liquid bromine and purified by a microdistillation technique. The supernate was reduced by ethanol and Re was extracted and purified by liquid/liquid extraction with *iso*-amylic alcohol and 2N HNO_3.

In order to achieve a complete digestion of refractory chromium spinel and associated platinum group alloys, we applied the Carius tube digestion method (Shirey and Walker, 1995) to the chromite sample. Approximately 0.05 g of sample powder, spikes, 0.2 ml of concentrated HCl and 0.4 ml of concentrated HNO_3 were frozen into Pyrex™ Carius tube. The tube was sealed and heated for about 16 h at 240 °C and the Os and Re were then extracted with the method described above.

It has been shown by Meisel et al. (2003) that the low-temperature acid digestion technique used in this study does not release all the Os from metamorphosed peridotite reference material. As a consequence, the ultramafic rocks measured in this study after low-temperature acid digestion, may have slightly higher Os contents together with lower Os isotope composition (Meisel et al., 2003). To check for such inconsistencies, duplicate measurements of one lherzolite (My 37) and one wehrlite (Nu 48) sample were carried out by Carius tube method (Shirey and Walker, 1995) at the Open University (see Table 2). The Os isotopic composition yield by both methods is exactly the same within the analytical error, and the Os concentration is only 1% higher for the lherzolite sample using the Carius tube method. The result in the isotopic composition can be explained by the fact that the interstitial sulphides are the main Os-bearing phase, and they are easily dissolved by the low-temperature acid digestion technique used here. Similar Os isotope systematics determined for unmetamorphosed peridotite xenoliths using acid digestion and Carius tube digestions have also been demonstrated by Shirey and Walker (1995) suggesting that both methods are equally efficient in extracting Os from unmetamorphosed ultramafic samples. It may be considered therefore that the Os isotope compositions reported here are reliable.

Whole-rock major and trace element concentrations were determined at the Service d'Analyse des Roches et des Minéraux (SARM) at the Centre de Récherche Pétrographiques et Géochimique (SRPG-CNRS, Nancy, France). Analyses of major elements were performed by ICP-AES after alkaline melting with lithium borate and nitric acid dissolution. The analytical error is 1–10% for the concentrations exceeding 1 wt.%, and 2–20% for element concentrations below 1 wt.%. Concentrations of trace elements were analysed by ICP-MS and show

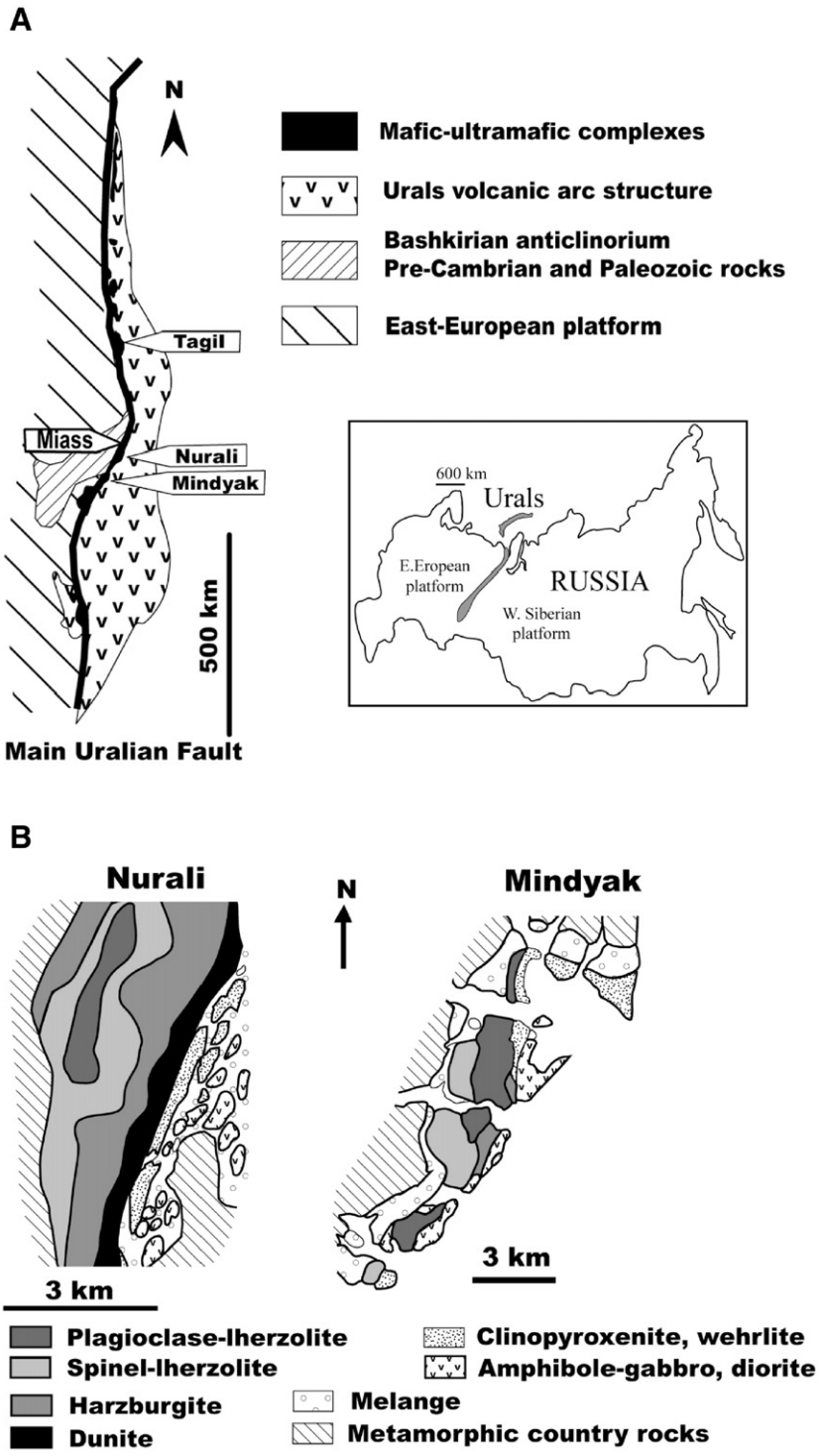

Fig. 1. (A) Schematic geological map of the Urals and location of the Nurali and Mindyak lherzolite massifs (modified after Garuti et al., 1997). (B) Schematic geological map of the lherzolite–harzburgite complexes Nurali and Mindyak (after Garuti et al., 1997).

variable precision and accuracy which strongly depend on element concentration in the samples. At a concentration level above 10 ppm (i.e., for most common concentrations of Co, Ni, Cr, and V), the precision and accuracy are better than 15%. Ga, W, Y and Ge (which show concentrations between 1 and 50 ppm in the

Table 1
Major (wt.%) and trace elements (ppm) compositions of the Nurali and Mindyak massifs

	My 29	My 33	My 30	My 31	My 37	My 38	My 39	My 40	My 41	My 28	My 32	My 34	My 35	My 36
	Hz	Hz	Lz	Lz	Lz	CPx	W	CPx	CPx	G	G	G	G	D
SiO_2	44.48	46.54	43.26	44.51	44.99	52.26	45.27	48.26	46.93	48.33	54.04	47.35	52.44	54.30
TiO_2	<0.05	<0.05	<0.05	0.10	<0.05	<0.05	0.22	0.23	0.27	0.65	0.41	0.64	0.67	0.53
Al_2O_3	1.28	1.81	2.29	3.39	2.14	3.39	2.70	2.97	3.41	16.05	16.16	19.98	16.11	14.45
FeO*	7.75	5.43	8.01	7.89	7.01	5.52	12.43	9.70	10.92	8.84	7.80	10.25	10.31	9.44
MgO	44.47	45.25	43.41	39.27	44.05	31.82	24.61	20.04	20.39	8.62	5.80	5.18	6.44	7.24
CaO	0.95	0.19	2.03	3.62	0.85	6.11	13.06	17.36	16.52	13.34	9.31	12.08	8.30	6.48
Na_2O	<0.05	<0.05	<0.05	0.14	<0.05	0.08	0.10	0.15	0.12	2.88	5.03	2.74	3.69	3.76
LOI	10.45	11.14	7.06	5.82	13.06	4.04	4.15	3.11	2.96	0.73	1.62	2.41	2.49	1.82
S	225	114	172	192	655	514	177	<100	<100	223	<100	154	1328	<100
V	39	39	50	69	46	114	242	261	317	270	190	325	292	331
W	0.50	0.17	0.78	1.30	0.34	1.54	1.09	1.84	1.21	2.25	2.35	1.53	1.71	1.15
Y	0.44	0.81	1.19	2.65	1.27	0.51	4.91	5.78	7.20	16.99	10.73	13.74	17.84	12.97
Cr	3041	2938	2698	3088	2844	6855	840	1828	825	256	83	25	37	139
Co	116	105	114	102	125	68	106	81	87	40	28	31	42	37
Ni	2333	2291	2307	1951	2432	1243	276	179	168	83	42	11	33	33
Cu	8	13	15	22	7	130	<1	17	<1	23	56	131	167	53
Zn	46	40	49	51	35	26	66	50	53	61	50	93	81	90
Ga	1.3	1.4	2.0	3.3	1.8	2.9	4.3	4.3	4.8	13.7	11.8	18.3	17.0	13.7
Ge	0.94	0.99	1.13	1.25	0.87	1.44	2.35	2.32	2.19	1.43	1.45	1.78	1.60	2.42
La	<0.05	<0.05	<0.05	<0.05	0.119	<0.05	0.139	0.274	0.203	1.158	1.664	6.944	1.708	9.023
Ce	<0.05	0.089	0.073	0.197	0.141	0.060	0.773	1.181	1.151	3.541	4.073	15.887	4.507	19.749
Pr	<0.04	<0.04	<0.04	0.045	<0.04	<0.04	0.201	0.266	0.267	0.603	0.615	2.255	0.735	2.701
Nd	<0.15	<0.15	<0.15	0.291	0.236	<0.15	1.600	1.981	2.243	3.518	3.227	11.248	4.107	10.434
Sm	<0.06	<0.06	<0.06	0.200	0.108	<0.06	0.674	0.830	0.868	1.498	1.092	2.784	1.538	2.674
Eu	<0.02	<0.02	<0.02	0.070	0.051	<0.02	0.248	0.286	0.336	0.566	0.425	1.033	0.610	0.892
Gd	<0.07	<0.07	0.112	0.231	0.247	<0.07	0.780	0.923	1.193	2.166	1.471	2.911	2.419	2.649
Tb	<0.01	0.012	0.021	0.058	0.035	<0.01	0.137	0.160	0.216	0.372	0.254	0.417	0.406	0.377
Dy	<0.05	0.102	0.183	0.399	0.173	0.076	0.918	1.195	1.214	2.659	1.665	2.291	2.790	2.259
Ho	0.017	0.036	0.036	0.096	0.047	0.015	0.206	0.244	0.281	0.620	0.399	0.558	0.646	0.461
Er	0.056	0.100	0.117	0.295	0.146	0.082	0.560	0.666	0.685	1.802	1.184	1.445	1.843	1.431
Tm	0.012	0.017	0.027	0.050	0.019	0.013	0.077	0.096	0.103	0.291	0.184	0.225	0.299	0.206
Yb	0.050	0.143	0.174	0.310	0.173	0.089	0.438	0.566	0.735	1.889	1.240	1.437	1.925	1.386
Lu	0.018	0.025	0.021	0.040	0.024	0.022	0.072	0.089	0.104	0.279	0.180	0.204	0.313	0.228
F	13	16	10		12									
F (Ni)	16	15	15		20									

All compositions recalculated to anhydrous values, converting all Fe_2O_3 to FeO (FeO*). (–) lower than detection limit.

Table 1 (*continued*)

	Nu 60	Nu 64	Nu 58	Nu 59	Nu 61	Nu 62	Nu 47	Nu 48	Nu 51	Nu 52	Nu 53	Nu 54	Nu 55	Nu 56
	Du	Du	Lz	Lz	Hz	Hz	W	W	W	G	G	G	G	D
SiO_2	40.19	40.34	44.01	44.77	44.13	44.10	51.75	46.67	51.22	42.51	45.50	41.61	41.91	55.15
TiO_2	<0.05	<0.05	<0.05	<0.05	<0.05	<0.05	0.06	<0.05	0.15	0.88	0.77	1.01	0.95	0.65
Al_2O_3	0.21	0.12	2.71	2.55	1.86	0.57	1.36	2.11	1.88	20.90	18.85	21.73	22.48	18.81
FeO*	7.75	7.32	7.85	7.75	7.78	8.12	4.37	7.67	5.28	10.82	7.58	11.98	12.03	8.00
MgO	50.63	51.25	41.66	41.62	43.45	45.72	22.15	40.30	20.32	6.02	8.16	6.24	5.20	3.96
CaO	0.17	<0.01	2.56	2.17	1.66	0.41	19.61	2.02	20.28	15.66	14.58	13.81	13.80	8.13
Na_2O	<0.05	<0.05	0.15	0.16	0.06	<0.05	0.12	0.16	0.17	1.15	1.45	1.39	1.64	2.89
LOI	13.39	14.38	3.73	5.21	5.58	12.05	2.48	8.68	0.61	3.46	2.08	2.96	2.72	1.92
S	<100	140	<100	<100	<100	147	419	590	<100	166	<100	<100	<100	<100
V	10	9	53	52	42	27	69	73	137	358	189	386	298	244
W	0.51	0.48	1.24	1.82	1.51	0.44	2.04	1.89	1.86	0.98	2.12	1.82	1.80	1.57
Y	<0.05	<0.05	1.33	1.49	0.88	0.08	1.66	1.15	3.24	25.35	19.13	28.27	28.72	19.10
Cr	3455	3549	2850	2486	2542	3251	2784	3208	2398	15	340	15	11	8
Co	128	125	102	104	110	123	47	100	47	30	45	32	23	21
Ni	2652	2602	1931	1983	2198	2560	230	1948	330	19	218	16	11	11
Cu	<1	<1	<1	64	11	<1	7	8	6	65	7	43	12	27
Zn	42	38	46	44	48	45	23	45	25	94	62	85	115	80
Ga	0.3	0.3	2.3	2.1	1.5	0.6	1.7	1.9	2.1	21.3	15.7	21.6	23.1	17.6
Ge	0.85	0.88	0.78	0.98	0.93	1.04	2.26	1.34	1.95	1.63	1.55	1.58	1.36	1.54
La	<0.05	<0.05	<0.05	<0.05	<0.05	<0.05	0.894	0.272	0.281	6.154	2.417	3.764	5.465	9.388
Ce	<0.05	<0.05	<0.05	<0.05	<0.05	<0.05	2.038	0.823	0.973	16.312	6.718	11.553	15.812	20.033
Pr	<0.04	<0.04	<0.04	<0.04	<0.04	<0.04	0.288	0.120	0.190	2.582	1.062	1.933	2.469	2.524
Nd	<0.15	<0.15	<0.15	<0.15	<0.15	<0.15	1.475	0.692	1.009	12.951	5.551	11.221	13.243	10.628
Sm	<0.06	<0.06	<0.06	<0.06	<0.06	<0.06	0.350	0.183	0.420	3.558	1.931	3.600	3.832	2.515
Eu	<0.02	<0.02	0.026	0.036	<0.02	<0.02	0.143	0.074	0.157	1.231	0.788	1.249	1.291	0.956
Gd	<0.07	<0.07	0.137	<0.07	<0.07	<0.07	0.446	<0.07	0.522	4.222	2.530	4.438	4.780	3.037
Tb	<0.01	<0.01	0.024	0.023	0.017	<0.01	0.044	0.024	0.087	0.669	0.450	0.706	0.724	0.495
Dy	<0.05	<0.05	0.148	0.198	0.125	<0.05	0.325	0.184	0.672	4.219	2.802	4.603	4.864	3.249
Ho	<0.01	<0.01	0.045	0.051	0.033	<0.01	0.062	0.042	0.127	0.962	0.672	0.975	1.025	0.666
Er	<0.04	<0.04	0.132	0.165	0.106	<0.04	0.176	0.124	0.334	2.552	1.852	2.660	2.834	2.053
Tm	<0.01	<0.01	0.026	0.027	0.012	<0.01	0.025	0.028	0.044	0.406	0.291	0.409	0.443	0.291
Yb	<0.03	<0.03	0.197	0.179	0.128	<0.03	0.175	0.170	0.319	2.869	1.979	2.650	2.930	2.058
Lu	<0.01	<0.01	0.028	0.029	0.024	<0.01	0.023	0.029	0.040	0.394	0.277	0.373	0.397	0.305
F	24	25	6	6	10	15								
F (Ni)	26	25	0	2	11	24								

samples studied) were analysed with an analytical error better than 15%. The REE concentrations (with a range between 0.1 an 15 ppm in the studied samples) were analysed with an analytical error better than 15% (except for the Dy, which had an analytical error of 20%). Analyses for the international standards used as well detection limits and analytical uncertainties in the CRPG laboratory at Nancy can be viewed in the Supplementary material.

Serpentine alteration is significant for the analysed peridotites, as evident from the large losses on ignition (up to 14%;Table 1). This was corrected for by recalculating the whole-rock analyses as anhydrous compositions. Total iron contents were also recalculated as FeO to facilitate comparisons with published analyses of peridotites.

5. Results

5.1. Major and trace elements

The whole-rock major and trace element concentrations for the Nurali and Mindyak mafic and ultramafic rocks are shown in Table 1. The Al_2O_3 and CaO contents of the peridotites are inversely correlated with MgO, which varies from 39.3 wt.% in the lherzolites up to 51.3 wt.% in the dunites from the Nurali massif (Fig. 2). The Mindyak ultramafics have Al_2O_3 contents ranging from 1.3 wt.% in the harzburgites up to 3.4 wt.% in the lherzolites, reflecting variable degrees of melt depletion. The Nurali peridotites have lower Al_2O_3 contents ranging from 0.1 wt.% in the dunites up to 2.6 wt.% in the lherzolites, possibly due to higher degrees of depletion.

Ni, Co and Cr concentrations in the peridotites are positively correlated with their MgO contents, consistent with their compatible behaviour during melting (e.g., Frey et al., 1985), whilst the abundances of V, Y (Fig. 3) and Ga (not shown) are inversely correlated with MgO reflecting their incompatible behaviour. The whole-rock major and trace elements composition of sample My 31 (plagioclase-bearing lherzolite) closely resembles that of primitive or undepleted mantle (e.g., Jagoutz et al., 1979; McDonough and Sun, 1995).

In TZ cumulates, major element distributions display variations that mainly reflect the modal olivine/clinopyroxene/orthopyroxene ratio, with a gradual increase in CaO contents (in pyroxene) concordant with decreasing MgO contents. There is a systematic increase in olivine and whole-rock Mg# across the Nurali transitional zone (from 77–87 up to 90–91), suggesting high degrees of melting in the mantle source (Pertsev et al., 1997). Moreover, the negative correlation between spinel Cr# and Mg# for associated rocks and minerals cannot be explained by fractional crystallisation from a single parental magma and must therefore indicate multi-stage

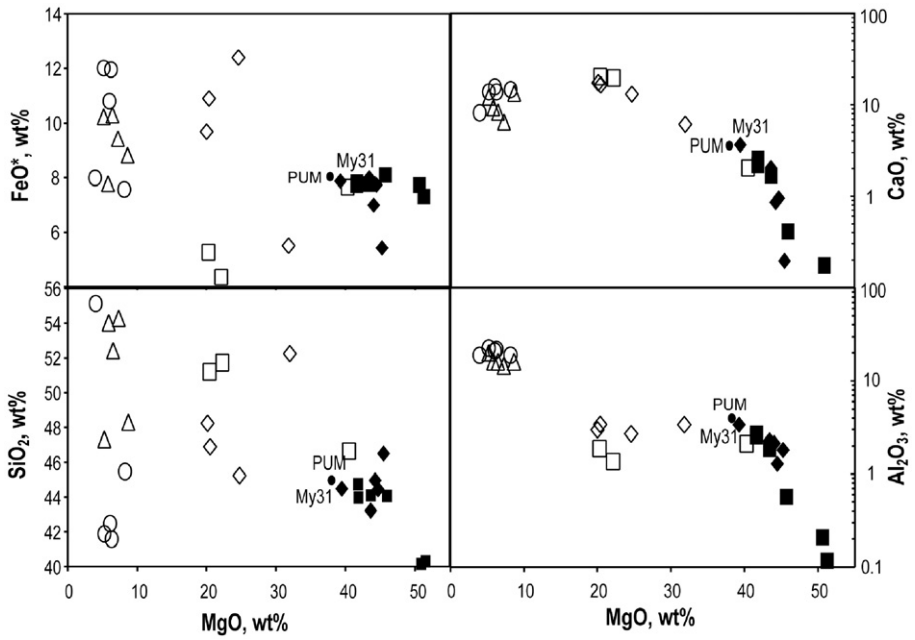

Fig. 2. Variations of whole-rock SiO_2, FeO, Al_2O_3 and CaO concentrations as a function of MgO in the Nurali peridotites (solid squares), Mindyak peridotites (solid diamonds), transition zone cumulates from the Nurali (open squares) and the Mindyak (open diamonds), as well as gabbro and mafic dykes from the Nurali (open circles) and Mindyak (open triangles) massifs; primitive mantle estimate is taken from (Jagoutz et al., 1979).

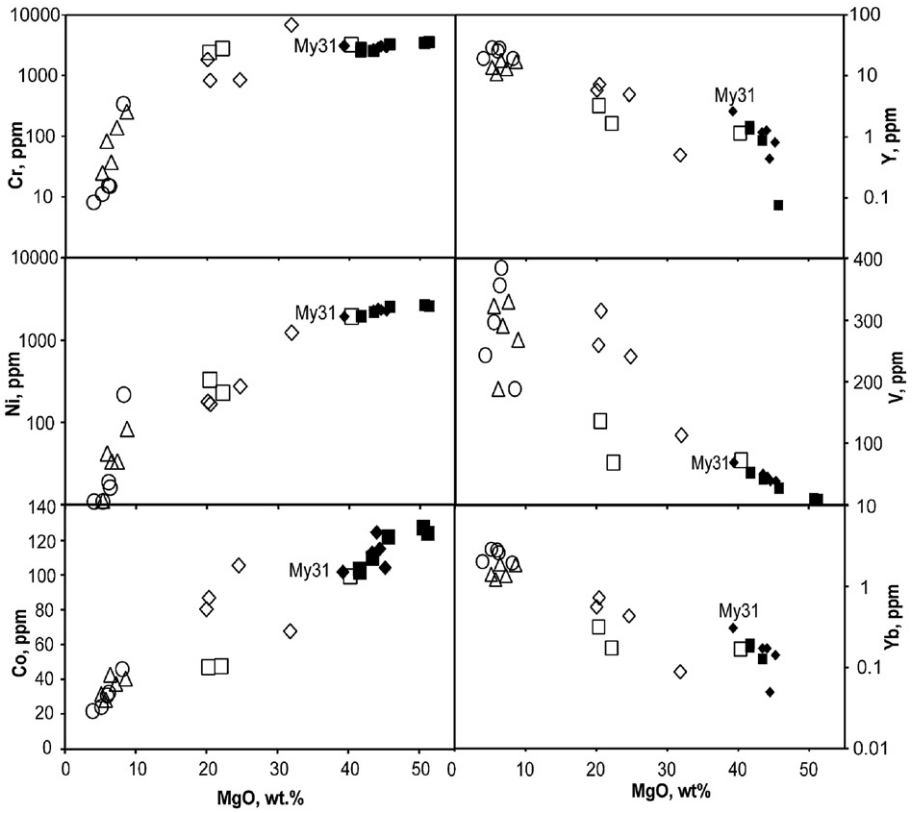

Fig. 3. Variations of whole-rock Co, Ni, Cr, Y, V, and Yb concentrations as a function of MgO in the Nurali and Mindyak mafic and ultramafic rocks. Symbols are given in the caption of Fig. 2.

magma intrusions. This statement can be supported by the lack of correlation between trace elements and MgO contents, except for the highly compatible elements such as Ni (Fig. 3). A rifting zone setting has been proposed by Pertsev et al. (1997) for such a multi-stage crystallisation without substantial magma differentiation.

5.2. Rare earth elements

The chondrite normalised whole-rock REE abundances of the peridotites, ultramafic cumulates, gabbro and diorites are shown in Fig. 4. Peridotites from the Mindyak massif are characterised by LREE depletion ($(Ce/Lu)_N$=0.20–0.24) and a flat to slightly fractionated HREE signature ($(Dy/Lu)_N$ ~ 0.7–1.01). The REE concentrations of the peridotites are inversely correlated with their MgO contents, as illustrated by the Yb-MgO trend in Fig. 3. The wehrlite and two clinopyroxenite samples from the Mindyak massif also show LREE-depleted signatures with $(Ce/Lu)_N$ ratio ranging from 0.43 to 0.53. These patterns are similar to those found in previous studies of peridotites and mineral separates from orogenic peridotite massifs (e.g., Loubet and Allègre, 1982; McDonough and Frey, 1989). Such REE patterns reflect differentiation from a LREE depleted mantle source which is typical of a mid-ocean ridge setting.

Gabbros and diorites from Mindyak massif form two distinct groups according to their REE patterns. The early gabbros (My 28, My 32, My 35) are characterised by LREE depletion with $(Ce/Lu)_N$ ratios from 0.51 to 0.91 (Fig. 4). A second group including a gabbro (My 34) and a diorite (My 36) with LREE-enriched patterns $(Ce/Lu)_N$ from 3.12 to 3.45, may represent crystallisation products of a separate magma injection from a more enriched source, which is more typical for a subduction zone setting.

Four from seven of the studied Nurali peridotites have REE concentrations lower than the detection limit. The HREE of three of the Nurali peridotites are fractionated relative to chondrite ($(Dy/Yb)_N$=0.73–0.49, with an abundance of 0.43 to 1.07 × chondrites). The LREE abundances in these peridotites are lower than the detection limit (0.05 μg/g) with $(Ce/Lu)_N$ ratio of <0.07. Such low Ce/Lu ratios cannot be explained by a single melting event, and is best accounted for by

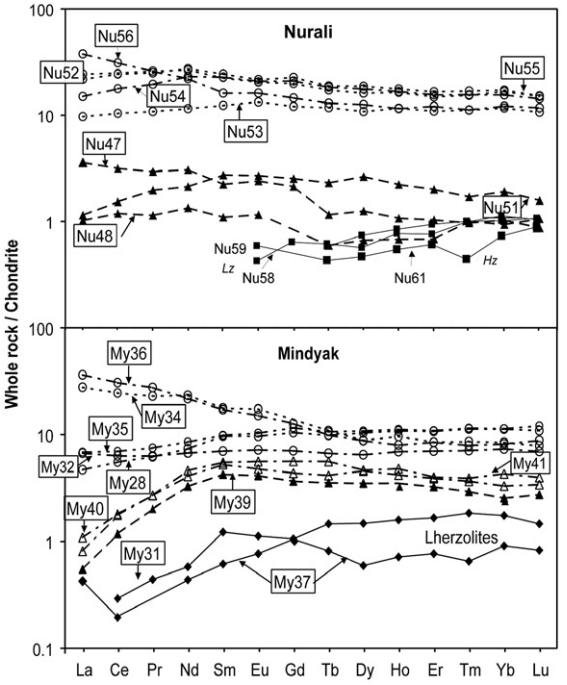

Fig. 4. Chondrite normalised REE profiles for the Mindyak lherzolites (solid diamonds), Nurali peridotites (solid squares), Nurali and Mindyak wehrlites (solid triangles), clinopyroxenites (open triangles), gabbros and diorites (open circles). Chondrite normalising values are from McDonough and Frey (1989).

multiple melting events leading to a progressive depletion in LREE. A similar conclusion has been drawn from mineral chemistry studies (Pertsev et al., 1997). The Nurali ultramafic cumulates, gabbro and diorites are characterised by a flat to slightly enriched REE patterns relative to chondrite with a $(Ce/Lu)_N$ ratios from 0.97 up to 3.6 (Fig. 4), indicating a fertile or slightly enriched source for the melt.

5.3. PGE systematics

The Ir-group PGE (Os, Ir, Ru) are highly compatible during mantle melting, and as a consequence they are not fractionated even by large degrees of melting up to 50% (Pearson et al., 2004). The fractionation of the less compatible Pd-group PGE (Rh, Pt, Pd) is usually expressed by the Pd/Os ratio, which can be considered as an index of PGE fractionation during petrogenetic processes. Since Os and Pd have chondritic abundances in the asthenospheric mantle, their normalised ratio is close to 1 in pristine mantle material. Moreover the Pd/Os ratio behaves similarly to the Re/Os ratio (Fig. 5 A) — it decreases with increasing degrees of melting and increases during magma differentiation.

The lherzolites and harzburgites from the Mindyak and the Nurali massifs have unfractionated primitive mantle-normalised PGE patterns (Garuti et al., 1997), with Pd/Os ratios ranging between 0.6 and 4.4 (25 for harzburgite from the fault zone). In contrast, the layered ultramafic cumulates from Mindyak and Nurali are depleted in Ni, Os, Ir and Rh. The PGE patterns have a positive slope with a degree of fractionation increasing upwards in the TZ sequence from wehrlites (Pd/Os=4.4–987) to pyroxenites (Pd/Os up to 1808) through to the gabbroic rocks (Pd/Os=44–3166).

The Pt anomaly (defined as $Pt/Pt^* = Pt_N/(Rh_N \bullet Pd_N)^{1/2}$) is often used as an index of PGE fractionation. This ratio is close to 1 in the primitive mantle, and is less than 1 for depleted PGE patterns such as in the Kempersai ophiolite massif (Southern Urals) or greater than 1 for enriched

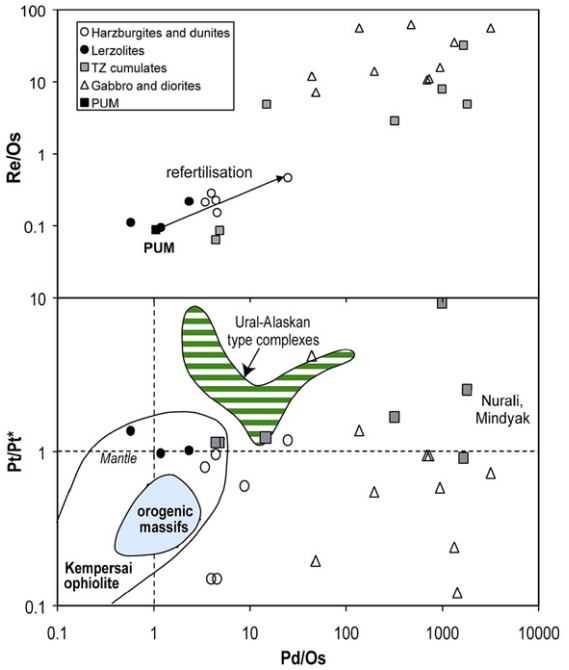

Fig. 5. (A) Plot of Pd/Os versus Re/Os for peridotites, transitional zone cumulates and mafic dykes from the Nurali and Mindyak massifs. Re and Os concentrations data are from this study, Pd concentrations are from Garuti et al. (1997). Primitive mantle estimate (PUM) is taken from Barnes et al. (1988) and Shirey and Walker (1998). (B) Plot of Pd/Os versus Pt/Pt* for whole-rock peridotites, transitional zone cumulates and mafic dykes from the Nurali and Mindyak massifs in comparison with the data from the Kempersai ophiolite massif, Southern Urals (Melcher et al., 1999), the Ural–Alaskan type mafic–ultramafic complexes (Garuti et al., 1997), and the orogenic lherzolite complexes from the Pyrenees, Ivrea zone, and Spain (data sources from Pearson et al., 2004; Garuti et al., 1997 and references therein). The Pt anomaly is calculated as follows: $Pt/Pt^* = Pt_N/(Rh_N \bullet Pd_N)^{1/2}$, where the PGE abundances are normalised relative to primitive mantle (Barnes et al., 1988).

Table 2
Re–Os concentrations and isotopic data for peridotites and Os-rich wehrlites from Mindyak and Nurali massifs

		Pt, ppb	Re, ppb	Os, ppb	$^{187}Os/^{188}Os$	$^{187}Re/^{188}Os$	γ_{Os}	T_{RD}, Ma
Mindyak							(500 Ma)	
My 29	Harzburgite	6.1	0.353	1.560	0.1249±4	1.096	−6.97	313
My 33	Harzburgite	34	0.508	1.093	0.1230±10	2.248	−16.25	595
My 30	Plg-lherzolite	7.3	0.702	3.224	0.1241±4	1.054	−7.27	432
My 31	Plg-lherzolite	6.6	0.376	3.982	0.1265±4	0.482	−1.54	75
My 37	Lherzolite	3.7	0.289	2.606	0.1195±5	0.537	−7.48	1110
My 37	CT duplicate		n.d.	2.635	0.1191±3			
Nurali								
Nu 60	Dunite	1	0.126	0.833	0.1217±8	0.733	−6.58	786
Nu 64	Dunite	1	0.272	0.961	0.1271±17	1.371	−6.49	–
Nu 61	Harzburgite	8	0.812	3.812	0.1222±3	1.031	−8.17	712
Nu 62	Harzburgite	4.8		0.955	0.1212±1	1.307	−10.80	860
KH-152	Chromite		0.432	9.610	0.1254±2	0.218	−0.07	239
							(1.25 Ga)	
Nu 48	Wehrlite	9.5	0.178	2.065	0.1294±4	0.411	1.47	–
Nu 48	Duplicate		0.146	2.274	0.1272±4	0.311	1.77	–
Nu 48	CT duplicate		n.d.	2.107	0.1291±3			
Nu 49	Wehrlite		0.380	2.371	0.1376±11	0.774	1.25	1685

Pt concentrations are from Garuti et al. (1997). Chromite KH-152 is chromitite within altered harzburgite (orthopyroxenite) xenoliths in wherlite. The γ_{Os} at 500 Ma (percentage difference between the Os isotopic composition of a sample and the average chondritic composition for a specified time) and rhenium depletion age (T_{RD}) are calculated according to Shirey and Walker (1998) using an average chondrite $^{187}Os/^{188}Os$ today of 0.1270, the average $^{187}Re/^{188}Os$ ratio of chondrites of 0.40186, and ^{187}Re decay constant ($\lambda^{187}Re$) of 1.666×10^{-11} year^{-1}. Rhenium depletion age has been calculated assuming that the $^{187}Re/^{188}Os$ ratio of peridotites is equal to zero at the time of melting. This approach allows late modification of the Re/Os ratio related to tectonic emplacement and alteration processes to be ignored.

PGE patterns such as in the Ural–Alaskan type complexes. The Nurali and Mindyak lherzolite massifs are characterized by Pt/Pt* close to the primitive mantle (Fig. 5 B). However, the residual peridotites from the Nurali and Mindyak complexes have systematically higher Pd/Os ratios than primitive mantle. This trend has been mainly attributed to Pd enrichment (Garuti et al., 1997), and by analogy with other peridotite massifs, may be considered to be a result of later basaltic melt percolation processes (Büchl et al., 2002), possibly associated with the re-activation of mantle peridotites during the Uralian island-arc development.

5.4. Os isotope systematics

5.4.1. Ultramafic rocks

Osmium and rhenium contents of the Nurali and Mindyak ultramafic rocks range from 0.8 to 4.0 ppb and from 0.13 to 0.81 ppb respectively (Table 2). The $^{187}Os/^{188}Os$ isotope ratios for the peridotites and Nurali chromites range from 0.119 to 0.126 ppb; this is typical of abyssal peridotites and orogenic lherzolite complexes, and is close to values for SCLM xenoliths from the Xing'an Mongolian Orogenic Belt and other peridotite xenoliths from continental rift zones, continental margins and oceanic regions (Shirey and Walker, 1998; Meisel et al., 2001; Wu et al., 2003; see Fig. 6). The measured $^{187}Re/^{188}Os$ ratios are higher than both depleted (0.06–1) and fertile (~0.4) mantle values (Shirey and Walker, 1998). The $^{187}Re/^{188}Os$ ratio could have been perturbed by late melt addition or alteration processes (Fig. 7A) and consequently cannot be used to infer an initial $^{187}Os/^{188}Os$ ratio. However, we can estimate a minimum

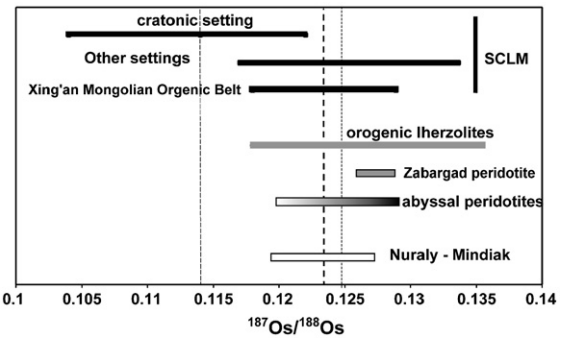

Fig. 6. Osmium isotope composition for the Nurali and Mindyak lherzolite massifs (this study) compared with present-day values for depleted mantle abyssal peridotites (Walker et al., 2002); sub-continental lithospheric mantle xenoliths: (a) from cratonic settings (Shirey and Walker, 1998), (b) young continental extensional rifts, oceanic regions, continental margins (Meisel et al., 2001), and (c) Xing'an Mongolian Orogenic Belt (Wu et al., 2003); orogenic lherzolite complexes (Reisberg et al., 1991; Roy-Barman et al., 1996); and lherzolite peridotites from Zabargad island, Red sea (modern rifting zone).

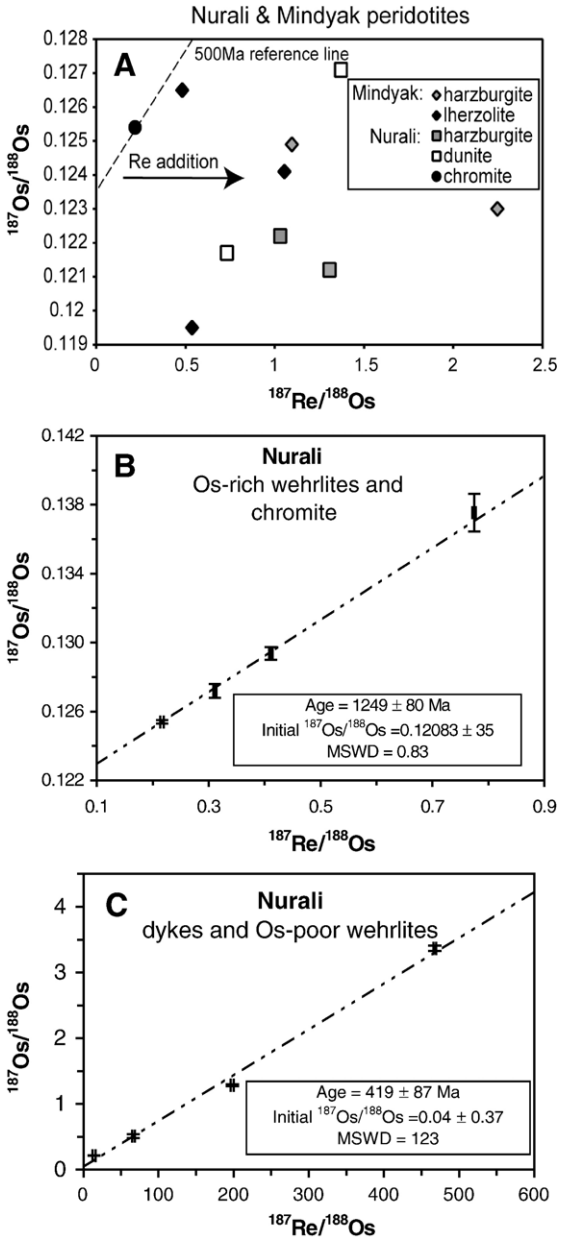

Fig. 7. Re–Os isochron diagrams for: (A) Nurali and Mindyak ultramafic rocks; (B) Nurali Os-rich wehrlites and chromite samples; (C) diabase-gabbro dykes and Os-poor wehrlites samples from Nurali massif.

age of Re depletion, assuming that the Re/Os ratio of the sample was reset to zero at the time of melting (for calculation method, see Shirey and Walker, 1998). The calculated rhenium depletion age for the Mindyak peridotites (except for lherzolite sample My 31) range from 313 to 1110 Ma (Table 2), possibly reflecting several episodes of melting. The rhenium depletion age for the Nurali peridotites (except for the upper dunite Nu 64) is Neoproterozoic showing a range in age from 712 to 860 Ma (see Table 2). The peridotites are also characterised by low γ_{Os} 500 Ma, ranging from −10.8 (−16.3 within the fault zone) up to −1.5, which is typical for SCLM xenoliths and lower than MORB and abyssal peridotites (Ellam et al., 1992; Shirey and Walker, 1998).

The chromite (KH-152) from the Nurali complex yielded a $^{187}Os/^{188}Os$ ratio of 0.125, which yields a melt extraction age of 520 Ma and chondritic initial ratio with γ_{Os} of −0.07.

5.4.2. Cumulates

The seven cumulate samples form two groups with respect to their osmium contents. The high Os cumulates include Nurali wehrlites with Os contents ranging from 2.07 to 2.37 ppb, and a Mindyak clinopyroxenite with an Os concentration of 0.81 ppb (Table 2). Four other wehrlites (My 39, Nu 47, NU 50, Nu 51) and another clinopyroxenite (My 40) have lower Os contents (between 4.2 and 50.4 ppt). Rhenium concentrations range from 62 ppt to 380 ppt for both groups, except for a clinopyroxenite sample with an extremely high Re content (~3.9 ppb, see Table 3). The cumulate rocks from the transition zones are characterised by elevated Re/Os ratios up to 55.7, which is much higher than for the harzburgites and the dunites (0.1–0.28).

The $^{187}Os/^{188}Os$ ratios for the Nurali wehrlites (0.128 to 0.138) are slightly higher compared with the peridotites. Two cumulates (Mindyak clinopyroxenite My 38 and Nurali wehrlite Nu 47) give high $^{187}Os/^{188}Os$ ratios from 0.638 up to 0.660. The $^{187}Os/^{188}Os$ ratios in low-Os cumulates vary between 0.173 and 0.224, which is close to what has been reported for the Beni-Bousera and Lanzo pyroxenites (Roy-Barman et al., 1996).

Three analyses of Os-rich wehrlites and one analysis of the chromite from the Nurali transition zone give an isochron with an age of 1249±80 Ma (MSWD=0.83) and an initial $^{187}Os/^{188}Os$ of 0.12083±0.00035 (Fig. 7 B), which is slightly higher than the average mantle value at that time and corresponds to a γ_{Os} value of 1.9. The supra-chondritic initial Os value, and the absence of a correlation between $^{187}Os/^{188}Os$ and 1/Os supports the idea that the correlation in ^{187}Re–^{187}Os isotope evolution diagram is a function of age rather than mixing.

5.4.3. Mafic rocks

The osmium contents of the mafic dykes and gabbros (1.5 to 112 ppt) are much lower than those of the ultramafics, while the rhenium contents (85 ppt to 2 ppb) are higher (Table 3). Whole-rock Re–Os systematics for the gabbros and diorites from the Mindyak massif define three straight-line correlations for $^{187}Os/^{188}Os$ versus $^{187}Re/^{188}Os$ (Fig. 8). The two

Table 3
Re–Os concentrations and isotopic data for cumulates and mafic dykes from Mindyak and Nurali massifs

	Lithology	Os ppt	Re ppt	$^{187}Os/^{188}Os$	$^{187}Re/^{188}Os$	Model T, Ma
Mindyak						
My 38	Clinopyroxenite	805.1	3931	0.638±3	25.2	1223
My 39	Wehrlite	7.8	62	0.173±	38.6	72
My 40	Clinopyroxenite+mgn	16.0	79	0.224±7	24.0	246
My 28	Gabbro dyke	19.2	212	0.569±	56.7	469
My 28	Duplicate	20.3	216	0.532±7	54.3	449
My 32	Gabbro dyke	3.8	213	2.94±2	377.7	446
My 34	Amph-gabbro	111.9	1335	0.919±14	49.3	964
My 35	Gabbro	21.3	1194	5.62±25	467.0	702
My 35	Duplicate	11.1	998	24.1±5	1797.4	795
My 35	Duplicate	15.4	1145	12.4±5	934.5	783
My 35	Duplicate	11.7	1029	28.7±5	2026.4	840
My 35	Duplicate	12.6	1121	22.8±7	1721.2	787
My 35	Duplicate	13.9	2057	27.9±5	3339.6	498
My 35	Duplicate	18.0	1589	10.3±5	1000.9	607
My 35	Duplicate	21.3	1194	5.6±2	467.0	702
My 35	Duplicate	14.1	2040	28.6±8	3330.3	511
My 35	Duplicate	11.5	1149	14.0±2	1418.3	585
My 35	Duplicate	18.6	1157	6.3±2	569.1	652
My 36	Diorite	6.9	110	1.46±5	90.0	889
Nurali						
Nu 47	Wehrlite	4.2	134	0.66±13	166.9	192
Nu 50	Wehrlite	40.5	708	0.1988±8	85.6	51
Nu 51	Wehrlite	50.4	144	0.214±2	14.0	382
Nu 52	Melanogabbro	1.5		3.37±4	467.8	415
Nu 55	Gabbro	3.0	185	1.014±8	345.2	154
Nu 54	Amph-gabbro	49.9	359	0.797±11	37.5	1073
Nu 53	Amph-gabbro	25.1	350	0.512±28	66.5	349
Nu 56	Diorite	2.4	86	1.286±13	198.0	351

Used abbreviations: amph=amphibole,; mgn=magnetite.
The model age corresponds to the age of separation from the chondritic mantle. It is calculated according to Shirey and Walker (1998) by extrapolation of the Os composition of the sample back in time using the measured $^{187}Re/^{188}Os$ ratio.

gabbro dykes cutting the mantle unit of Mindyak massif yield an age of 447±20 Ma (MSWD=0.25) and an initial $^{187}Os/^{188}Os$ of 0.121±0.064, close to mantle values (Fig. 8 A). The second straight-line correlation obtained for 6 different batches of the gabbro sample (My 35) is almost parallel to the first one and gives a best-fit age of 476±19 Ma (MSWD=1.5) with an initial $^{187}Os/^{188}Os$ isotope ratio of 1.94±0.37, which is much higher than typical mantle material (Fig. 8 B). One diorite and two gabbro samples from the upper part of Mindyak massif, and a clinopyroxenite from the transition zone, define an isochron with a best-fit age of 804±37 Ma (MSWD=2.8) and a poorly defined initial $^{187}Os/^{188}Os$ ratio of 0.07±0.65 (Fig. 8 C). It is notable that the diorite (My 36) and gabbro (My 34) samples are both enriched in LREE with $(Ce/Lu)_N$ ratios between 3.12 and 3.45 (Fig. 4); these possibly represent crystallisation products from a separate magma injection from a more fertile source.

Surprisingly, most radiogenic analyses of the third (Fig. 8 C) and second (Fig. 8 B) best-fit correlations correspond to the batches of the same gabbro sample (My 35). One interpretation for this could be that these gabbros were intruded later and interacted with older mafic material during emplacement; this would explain their radiogenic initial $^{187}Os/^{188}Os$.

The gabbro, diorite and wehrlite whole-rock samples from Nurali massif define a weak correlation with an age of 419±87 Ma (MSWD=123) and an initial $^{187}Os/^{188}Os$ ratios of 0.04±0.37 (Fig. 7 C).

5.5. Sm–Nd isotope systematics

The mafic–ultramafic rock samples from Mindyak and Nurali massifs were analysed for Sm–Nd systematics in order to complement the Re–Os data (Table 4). The peridotites from the Nurali massif (except for the harzburgite Nu 61) have very low Nd concentrations with a range from 1 to 5 ppb, which is similar to the highly depleted Voykar and Kempersay ophiolites (Sharma and Wasserburg, 1996). These low Nd contents do not allow precise isotopic measurements using our method. The Sm

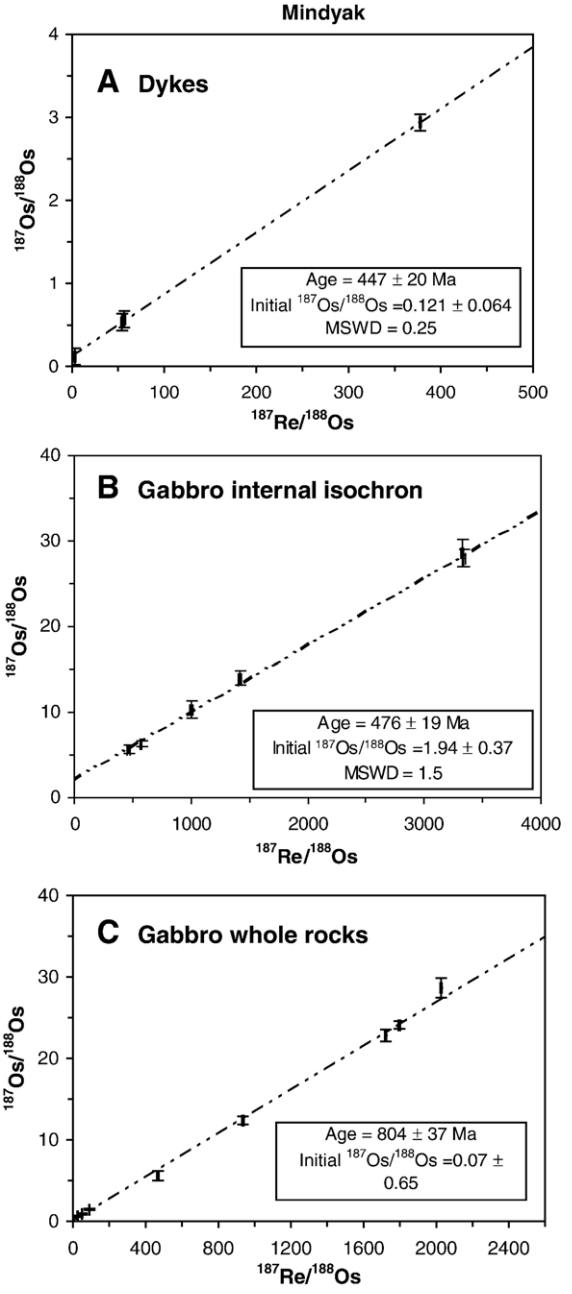

Fig. 8. Re–Os isochron diagram for Mindyak gabbro and diorites. There are at least three correlations. (A) Re–Os isochron diagram for Mindyak dykes cutting lower mantle units (My 28–1, My 28–2, My 32); the harzburgite sample (My 29) is shown; (B) internal isochron for the gabbro siample (My 35) established with 5 batches of the same powder; (C) Re–Os isochron diagram for Mindyak upper gabbros and diorites (My 34, My 35 (5), My 36) and clinopyroxenite (My 38).

and Nd concentrations in Mindyak ultramafic rocks on the other hand are higher, ranging from 17 to 169 ppb and 31 to 337 ppb, respectively (Table 4). As expected, the cumulates have even higher Sm (25–739 ppb) and Nd (62 ppb–1.8 ppm) contents.

The $^{147}Sm/^{144}Nd$ and $^{143}Nd/^{144}Nd$ isotopic ratios of the peridotites, cumulates and gabbros show an inverse correlation with $(Ce/Yb)_N$, reflecting variable degrees of melt-induced fractionation in the residual peridotites (Fig. 9). However, the Sm–Nd isotope ratios of the harzburgite (sample My 33) are lower than those of the associated lherzolites (see Fig. 9); this is opposite of what may be expected from partial melting, and might instead be attributed to a melt percolation event. Indeed, these low isotopic ratios may be modelled by the addition of about 3 to 5% of basaltic melt for the highest $(Ce/Yb)_N$ and lowest Nd isotope ratios (Fig. 9).

The analyses of the Mindyak peridotites define a linear array in a ^{147}Sm–^{143}Nd isochron diagram (Fig. 10 A). A best-fit line through the six points gives an age of 882± 83 Ma with an MSWD=1.4 and an initial $^{143}Nd/^{144}Nd$ of 0.51172±0.00016, which corresponds to an initial ε_{Nd} value of +3.8 (ε_{Nd} expresses the difference between the initial $^{143}Nd/^{144}Nd$ ratio of the measured sample and the corresponding value of this ratio in a chondritic reservoir at the time the rock formed). This age is similar to the Re–Os isochron age for the gabbros from the same massif, and ~350 Ma younger than the Re–Os age of 1249±80 Ma obtained for the Nurali wehrlites and chromite.

Five whole-rock analyses for the Mindyak gabbros form an isochron with an age of 540±18 Ma (MSWD=0.90), an initial $^{143}Nd/^{144}Nd$ ratio of to 0.512263±0.000024, and an initial ε_{Nd} value of +6.3 (Fig. 10 B). This age is distinct from the Re–Os age for the same gabbros (804± 37 Ma). Moreover, there is a correlation between Nd concentrations and Nd isotope composition (not shown) for both the upper gabbro and mafic dykes, suggesting that the later melt percolation event has affected their Nd isotope compositions. In this sense, this relationship could be considered as a mixing line and its age significance may be more difficult to establish.

The peridotite, transition zone cumulates, upper gabbro and mafic dykes of the Nurali massif define two straight-line correlations with best-fit ages of 1000 Ga (initial ε_{Nd} value of +8), and 390 Ma, (initial ε_{Nd} value of +5.2) (Fig. 11). These correlations may represent mixing lines, and possibly indicate that a late melt percolation event has disturbed the Sm–Nd isotopic systematics.

6. Discussion

6.1. Origin of the lherzolite complexes

Orogenic lherzolites have often been interpreted as pieces of the continental lithospheric mantle that have

been tectonically emplaced into the crust (e.g., Reisberg et al., 1991). However, an alternative hypothesis arguing for an ocean crust origin for orogenic lherzolites has been proposed by Boudier and Nicolas (1985). They described orogenic lherzolites as an ophiolite subtype, which differs from the more common harzburgite subtype in that it is characterised by a thinner crustal section and a direct contact with metamorphosed continental crust. As suggested by these authors, orogenic lherzolites might therefore be associated with transform faults, or very slow spreading centres, where the lithospheric front penetrates 20–30 km into the mantle below.

On the basis of REE and Sr–Nd data, Bodinier et al. (1991) have concluded that orogenic lherzolites represent a MORB-type mantle. The Os isotope data of Roy-Barman et al. (1996) illustrate that orogenic lherzolite complexes are characterised by $^{187}Os/^{188}Os$ ratios close to that of abyssal peridotites and that they could indeed represent MORB type mantle. Radiogenic $^{187}Os/^{188}Os$ ratios of associated pyroxenites suggest that they may represent old delaminated oceanic crust (Roy-Barman et al., 1996). Furthermore, the Re/Os ratios of several orogenic lherzolite massifs have been perturbed, and consequently yield unrealistic Os model ages of up to 7 Ga. If one uses an initial $^{187}Re/^{188}Os$ ratio equal to 0, the calculated age is much younger (up to 1.2 Ga), and is similar to Nurali and Mindyak lherzolite complexes. Moreover, the pyroxenite layers found in orogenic lherzolites have been argued to represent recycled subducted oceanic crust (e.g., Hamelin and Allègre, 1988). Alternatively, Pearson et al. (1993) suggest that many of the pyroxenite layers in the Beni-Bousera massif are in fact high-pressure crystal segregates from melts of altered oceanic crust.

In what follows, we use our new isotope observations to identify the origin of the Nurali and Mindyak massifs.

6.2. Melting and refertilisation

The majority of the studied Urals peridotites (except for two dunite samples) plot on a $MgO–Al_2O_3$ diagram (Fig. 12 B) close to the model partial melting trend

Table 4
Sm–Nd isotopic data from Mindyak and Nurali massifs

Sample ID		Sm, ppm	Nd, ppm	$^{147}Sm/^{144}Nd$	$^{143}Nd/^{144}Nd$	T Nd, Ma	ε_{Nd}
	Mindyak						(900 Ma)
My 29	Harzburgite	0.017	0.032	0.2635	0.51329±14	1487	5.05
My 29	Replicate	0.017	0.032	0.2635	0.51325±10	1395	4.26
My 33	Harzburgite	0.040	0.124	0.1972	0.51283±8	–	3.70
My 33	Replicate	0.039	0.101	0.2034	0.51286±9	–	3.53
My 30	Plg-lherzolite	0.033	0.042	0.3907	0.5140±1	1075	4.38
My 31	Plg-lherzolite	0.169	0.337	0.3009	0.51346±2	1208	4.13
My 37	Lherzolite	0.182	0.237	0.4718	0.51298±6	191	
My 38	Clinopyroxenite	0.026	0.062	0.2502	0.51305±13	1181	
My 39	Wehrlite	0.561	1.294	0.2728	0.513078±11	882	
My 40	Clinopyroxenite	0.739	1.837	0.2484	0.513040±4	1185	
							(540 Ma)
My 28	Gabbro dyke	1.450	3.711	0.2412	0.513114±2	1627	6.22
My 32	Gabbro dyke	1.125	3.388	0.2049	0.512991±5	–	6.32
My 34	Amph-gabbro	2.663	11.103	0.1476	0.512782±3	449	6.20
My 35	Gabbro	1.507	4.125	0.2255	0.513058±3	2211	6.20
My 36	Diorite	2.365	10.789	0.1353	0.512753±11	286	6.49
	Nurali						
Nu 61	Harzburgite	0.030	0.031	0.5905	0.513809±99	454	
Nu 48	Wehrlite	0.148	0.589	0.1556	0.512822±13	685	
Nu 47	Wehrlite	0.364	1.430	0.1571	0.512839±2	780	
							(390 Ma)
Nu 51	Wehrlite	0.421	1.142	0.2277	0.512979±4	1671	5.11
Nu 52	Melanogabbro	3.282	12.489	0.1622	0.512819±1	802	5.25
Nu 53	Amph-gabbro	1.800	5.546	0.2003	0.513068±2	–	8.24
Nu 54	Amph-gabbro	3.676	12.076	0.1879	0.512883±2	–	5.23
Nu 55	Gabbro	3.815	13.724	0.1716	0.512874±3	1444	5.73
Nu 56	Diorite	2.667	10.993	0.1497	0.512783±1	474	5.18

The Nd model ages are reported relative to bulk Earth evolution, using $^{143}Nd/^{144}Nd$ ratio of 0.512638 and $^{147}Sm/^{144}Nd$ ratio of 0.1967 for the CHUR. The meaningless Nd model ages (T_{DM}=−) show open system behaviour.
For rocks description see Tables 1 and 2.

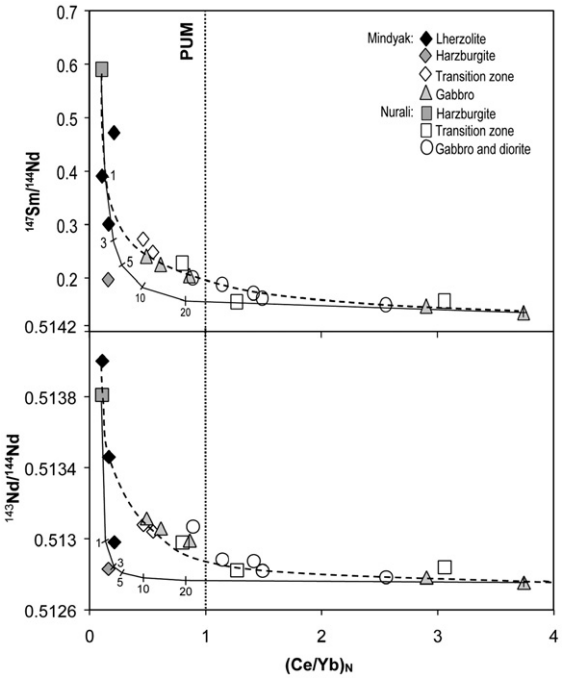

Fig. 9. $(Ce/Yb)_N$ ratio versus (A) $^{147}Sm/^{144}Nd$ and (B) $^{143}Nd/^{144}Nd$ ratios for peridotites, ultramafic cumulates, gabbros and diorites from the Nurali and Mindyak massifs. Mixing line between most depleted harzburgite sample from the Nurali massif and most enriched gabbro sample from the Mindyak massif is shown.

proposed by Niu (1997), and within a melting grid calculated for the FeO–MgO contents (Fig. 12 A). However, recent studies have indicated that the refertilisation of the upper mantle by the intrusion of mantle melts accompanied by melt/peridotite matrix interaction modify its chemical composition (e.g., Becker et al., 2001; Büchl et al., 2002). To determine the percentage of silicate melt addition, we have calculated a simple binary mixing trend between the most refractory peridotites samples from both the Nurali and Mindyak massifs; these are characterized by the lowest Al_2O_3 and highest MgO contents, and the basaltic melt after 30% of melting (the basaltic melt composition is taken from the experiments of Hirose and Kushiro (1993) for melting at 30 kbar). Fig. 12 shows that the observed major element compositions are consistent with both partial melting and refertilisation models. However, refertilisation is unlikely to be the dominant process because several observations argue against a significant amount of trapped silicate melt in peridotites: (1) the composition of Nurali and Mindyak peridotites are no more fertile than undepleted mantle, (i.e. the limited extent of trapped melt does not exceed the initial melt depletion); (2) the harzburgites and dunites from both Nurali and Mindyak massifs are more depleted in Al_2O_3 and more enriched in MgO compared to the lherzolites (this is more consistent with partial melting processes rather than Al_2O_3-rich melt addition); (3) LREE enrichment leading to U-shaped patterns, typical for later melt percolation and/or metasomatic events (e.g., Melcher et al., 1999), are not observed in the studied peridotites; and (4) the isochronous relationships established for the Mindyak peridotites also argue that parent–daughter element fractionation is mainly caused by partial melting and were not significantly disturbed by later melt percolation processes. Thus, even though local melt percolation might have occurred, major element compositions were not significantly changed as a result.

Despite the minor scatter around the melting trend, the major and trace element compositions of peridotites together with their REE patterns are consistent with an origin by partial melting of a fertile protolith. To estimate the degrees of melt extraction, the bulk MgO and FeO contents of the peridotites may be used (Frey et al., 1985). The proportion of melt extracted from the

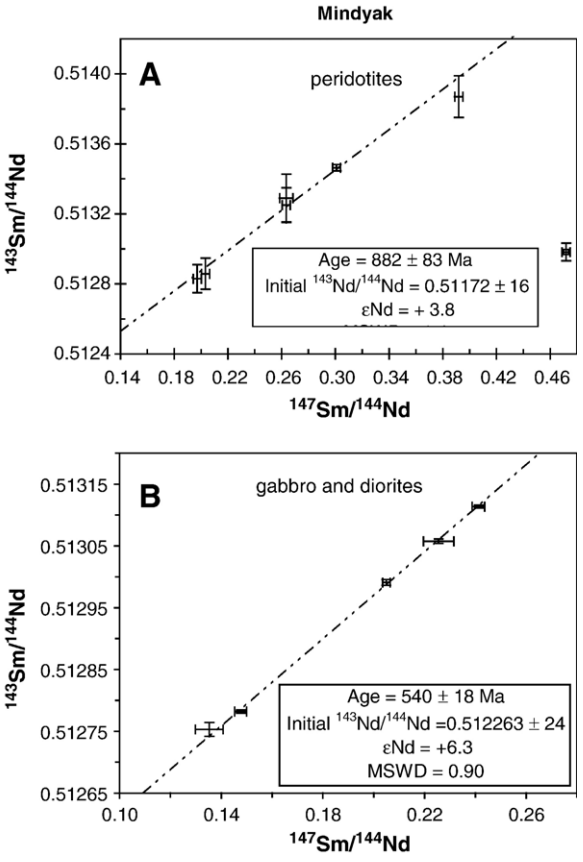

Fig. 10. Sm–Nd isochron plot for whole-rock samples from the Mindyak massif: (A) peridotites; (B) gabbro and diorites.

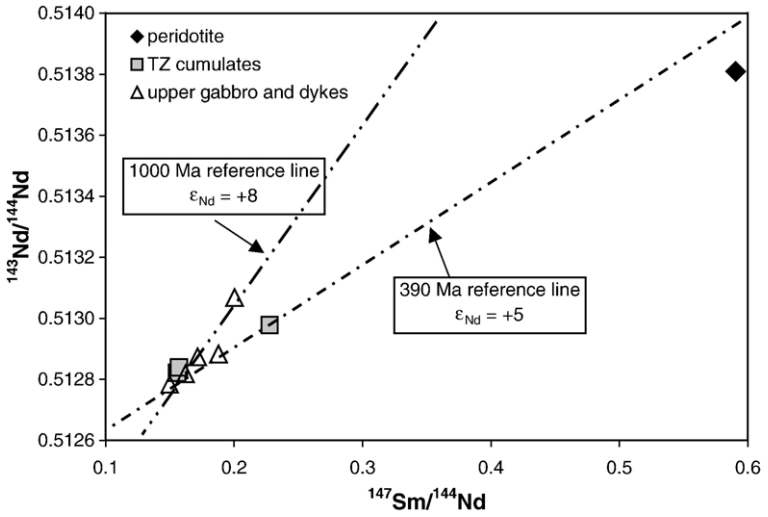

Fig. 11. Sm–Nd isochron plot for whole-rock gabbro and diorite samples from the Nurali massif.

Urals peridotites was estimated using the average olivine composition of ~ 0.91 (Scarrow et al., 1999), the olivine/melt exchange coefficient K_D of 0.35 (following Frey et al., 1985), and initial whole-rock MgO–FeO contents similar to that of sample My 31 (MgO = 36.76 wt.% and FeO = 7.39 wt.%), which is a lherzolite sample closest to the composition of primitive mantle (see Figs. 2 and 3). The calculated degrees of melt depletion for the Mindyak peridotites range from 6 to 12%, and to 25% for the dunites in the upper part of the Nurali massif (Table 1).

Furthermore, the degree of melting may also be estimated using the variation in concentration of highly compatible trace elements such as Ni in peridotites (for calculation method see Frey et al., 1985). Assuming an initial Ni content to be that of the lherzolite My 31 (1826 ppm), we obtain a similar range of degrees of melting (up to 26%) for the dunite samples from the Nurali massif (see Table 1). It may thus be assumed that the Mindyak and Nurali peridotites are characterised by moderate degrees of melt depletion not exceeding 20% for the lherzolites, and up to ~25% for the dunites in the

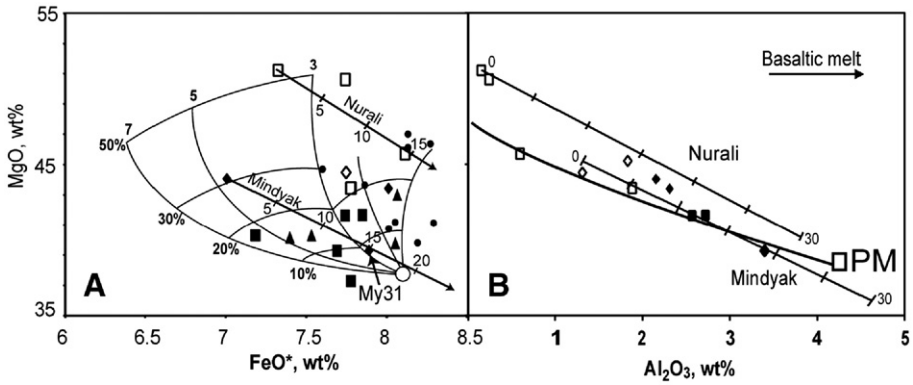

Fig. 12. (A) FeO–MgO and (B) Al_2O_3–MgO (anhydrous basis) diagrams for the Nurali lherzolites (solid squares) and harzburgites (open squares), the Mindyak lherzolites (solid diamonds), harzburgites and dunites (open diamonds), in comparison with the lherzolites from the Kraka massif (solid triangles, data from Savelieva et al., 1997) and the Beni-Bousera (solid circles) peridotites from Morocco (data from Pearson et al., 2004). (A) The melting grid outlines the expected composition of melt residues and is contoured for percent of melt extracted (in 10% intervals) at different melting pressures, in GPa (Walter, 2003). (B) The calculated fractional melting trend for residues from polybaric (2.5–4 Ga) fractional melting of fertile spinel lherzolite is shown by the solid black line (Niu, 1997). The refertilisation trends for the addition of up to 30% basaltic melt to a depleted harzburgite mantle composition (crosses placed at 5% interval) are shown on both diagrams, assuming simple two-component mixing. Basaltic melt composition taken from the experiments of Hirose and Kushiro (1993) for melting at 30 kbar. Depleted mantle composition is taken as the mean of the Mindyak harzburgite samples My 29 and My 33 and the dunite sample Nu 64 from the Nurali.

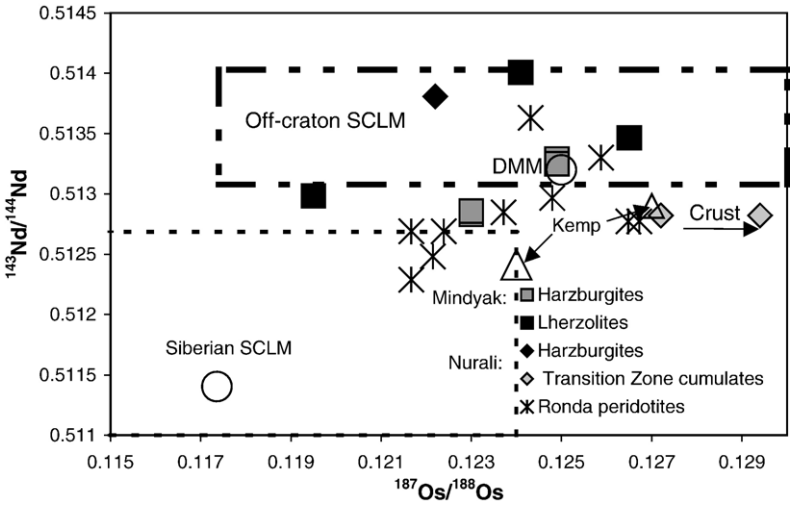

Fig. 13. The $^{187}Os/^{188}Os$ versus $^{143}Nd/^{144}Nd$ plot showing the present-day isotopic composition of the Nurali and Mindyak peridotites and ultramafic cumulates in comparison with that of the Kempersai ophiolite (Melcher et al., 1999) and the Ronda lherzolite massif (Reisberg et al., 1991). The field of the Archean lithospheric mantle from the Siberian craton (data from Pearson et al., 1995) and off-craton lithospheric mantle (data from Pearson et al., 2004; Ionov et al., 2005, median composition is shown by open circle), as well as the average depleted mantle composition (Shirey and Walker, 1998; Workman and Hart, 2005) are shown.

upper part of the Nurali mantle unit. This degree of depletion can be further argued based on the strong LREE depletion of the Nurali peridotites together with very high $^{147}Sm/^{144}Nd$ ratio (Table 4) which are similar to that of the highly depleted Voykar ophiolite massif in the Northern Urals (Sharma and Wasserburg, 1996). Such variable degrees of depletion may be explained by multiple melt extraction events. The degree of melting of the Urals peridotites is slightly lower than that estimated for the Ronda massif in Spain (>30%, Frey et al., 1985) and similar to that of the Pyrenean peridotites (>25%, Burnham et al., 1998).

However, the variation of some incompatible and platinum group elements are inconsistent with a simple partial melt extraction model. For example, the lower Sm/Nd and higher Re/Os and Pd/Os ratios in Mindyak harzburgites (Figs. 5, 9) compared with the associated lherzolites may be the result of the later melt-extraction–melt/fluid-rock interaction events, possibly in a supra-subduction zone setting. The absence of well-established correlations between the Os isotope compositions and fertility indexes such as Al_2O_3 and Yb contents in the peridotites also suggests that metasomatism and melt percolation processes may have affected the harzburgites.

6.3. Depleted or lithospheric mantle origin

There are two main views on the origin of the Urals lherzolite complexes: Savelieva et al. (2002) suggest that they are derived from weakly depleted oceanic mantle (DMM) whereas Garuti et al. (1997) suggest that they are derived from the sub-continental lithospheric mantle on the basis of the PGE abundances. The lithospheric mantle origin can be effectively resolved using the Re–Os isotope systematics. The unique Os isotope signature of the sub-continental lithospheric mantle results from the removal of incompatible Re during mantle extraction and the subsequent development of unradiogenic $^{187}Os/^{188}Os$ isotope compositions with γ_{Os} values down to −17 for the on-cratonic Archean lithospheric mantle (Shirey and Walker, 1998).

In order to compare our data with that of the Archean lithospheric mantle and the Urals ophiolites, we use the present-day $^{187}Os/^{188}Os$ vs. $^{143}Nd/^{144}Nd$ plot (Fig. 13). The Archean lithospheric mantle composition may be inferred from the studies of peridotites xenoliths from the Siberian craton (Pearson et al., 1995), which was originally attached to the Baltica craton in the Archean time (Khain et al., 2003). Fig. 13 shows that the $^{143}Nd/^{144}Nd$ and $^{187}Os/^{188}Os$ ratios of the studied lherzolite massifs are consistently higher than that of the highly refractory peridotitic xenoliths from the Siberian SCLM. Moreover, the Os abundances in the studied peridotite do not exceed 4 ppb (Table 2), which is lower than the average Os content of 4.2 ppb for the Archean lithospheric mantle (Pearson et al., 2004).

The Os and Nd isotope composition of studied peridotites corresponds to that of other Urals ophiolites (Kempersai ophiolite, Melcher et al., 1999) and of the

average depleted mantle (Shirey and Walker, 1998). The Nd–Os isotope systematic of the Mindyak peridotites together with their REE patterns (Fig. 4) are consistent with an origin by partial melting of already depleted protolith, which can be identified with a MORB-like mantle source. Two mafic samples with enriched REE patterns may further indicate that the Mindyak mantle section was subducted.

The combined Os and Nd isotope compositions of the studied Urals peridotites plot within the field of off-craton Proterozic lithospheric mantle, together with the Xing'an Mongolian Orogenic Belt (Wu et al., 2003) and Baikal rift in Siberia (Pearson et al., 1995; Ionov et al., 2005). The nearly chondritic initial $^{187}Os/^{188}Os$ ratios and γ_{Os} of +1.9 for the Nurali cumulates together with their flat to enriched REE patterns are indicative of a fertile to slightly enriched parental magma (see Fig. 4). Similar flat to LREE-enriched patterns were reported for the peridotitic xenoliths from the Xing'an Mongolian Orogenic Belt (Wu et al., 2003). Moreover, the average Os content of the studied Urals peridotites (2.1 ppb) is similar to the average off-craton lithospheric mantle (~2 ppb) (Pearson et al., 2004).

The Mesoproterozoic Re–Os age of ~ 1.25±0.08 Ga for the banded cumulates and chromite from the Nurali massif suggests that these cumulates were formed first by partial melting of a peridotitic upper mantle followed by fractional crystallisation in magma conduits. Pertsev et al. (1997) have proposed that this partial melting event was due to the injection of several magma batches in a rift zone setting. Such an epicontinental rifting event was established along the western slope of the Southern Urals at that time (see next section).

The re-activation of Nurali massif in the Middle Paleozoic at ~400 Ma is suggested by our combined Re–Os, Sm–Nd data set as well as by previous U–Pb dating of mafic dykes (Fershtater et al., 2000). This would imply that the Nurali massif would have survived for about 850 Ma. The most likely hypothesis was that it was incorporated in the lithospheric mantle beneath the passive margin of the Baltica proto-continent. Indeed, rifting or subduction processes may have led to the isolation of the ancient Archean lithospheric mantle from tectonically active zones, and its replacement by younger sub-continental lithospheric mantle (SCLM) derived from the convecting upper mantle, as has been suggested for the northeastern China (Wu et al., 2003) where lithospheric model ages range between 1.2 and 0.4 Ga. The Proterozoic Re–Os age of the Nurali ultramafic cumulates corresponds well to the age of the country rocks (see next section), which is a typical feature of the age relationships between SCLM and the overlying crust for most of Proterozoic and Phanerozoic regions (e.g., Wu et al., 2003). Moreover, the Os isotopic composition and Os model ages of the Nurali peridotites are similar to the peridotitic xenoliths from the Xing'an Mongolian orogenic belt (Fig. 6), which represents the south-eastern extension of the Central Asian fold belt (Uralian–Mongolian belt in the Russian literature). Thus, the Nurali massif may represent a piece of lithospheric mantle beneath the proto-Uralian orogenic zone, which has replaced the original Archean SCLM at the passive margin of Baltica.

The multi-stage development of Nurali massif is somewhat comparable to the Zabargad lherzolite massif, in the Red Sea (Brueckner et al., 1995). This massif was differentiated from a depleted mantle source about 700 Ma, and was then incorporated into the sub-continental Red Sea mantle lithosphere. It was then uplifted at a shallow crustal level during a recent Red Sea rifting event (~30 Ma ago). In the case of the Nurali massif, these events happened more than 400 Ma ago before the Urals chain formed.

6.4. Geodynamic implications for proto-Urals development

6.4.1. Mesoproterozoic

Around 1350 Ma ago, a rifting event was initiated, accompanied by the formation of volcano-sedimentary complexes, granite massifs and layered mafic intrusions along the western slope of the Southern Urals (Bashkirian anticlinorium). Some rift-related mafic dykes of similar age (~1350 Ma) within the Beloretzk metamorphic complex, on the eastern part of the Bashkirian anticlinorium have been dated by the Pb/Pb-single zircon method (Glasmacher et al., 2001). The formation of the Berdyaush rapakivi granite massif near the town of Miass (~1.354±0.2 Ga, Rb/Sr and U–Pb isotope data) is also inferred to have taken place in a similar continental rift setting (Koroteev et al., 1997).

It seems likely then the isolation of the Nurali ophiolite from the convective mantle is associated with rift basin development of a passive margin which extended along the eastern edge of the East European (Baltica) Craton (Fig. 14). Similar rifting regimes, suggested to exist at the same time along the passive margins of the Siberian and Kazakhstan–Tarim plates (Khain et al., 2003), may be related to the break-up of the large Mezoproterozoic Eurasian continent into Baltica and Siberia, followed by the opening of an oceanic basin at ~ 1200 Ma. The earliest records of oceanic crust along the Siberian margins appear at 1035±92 Ma.

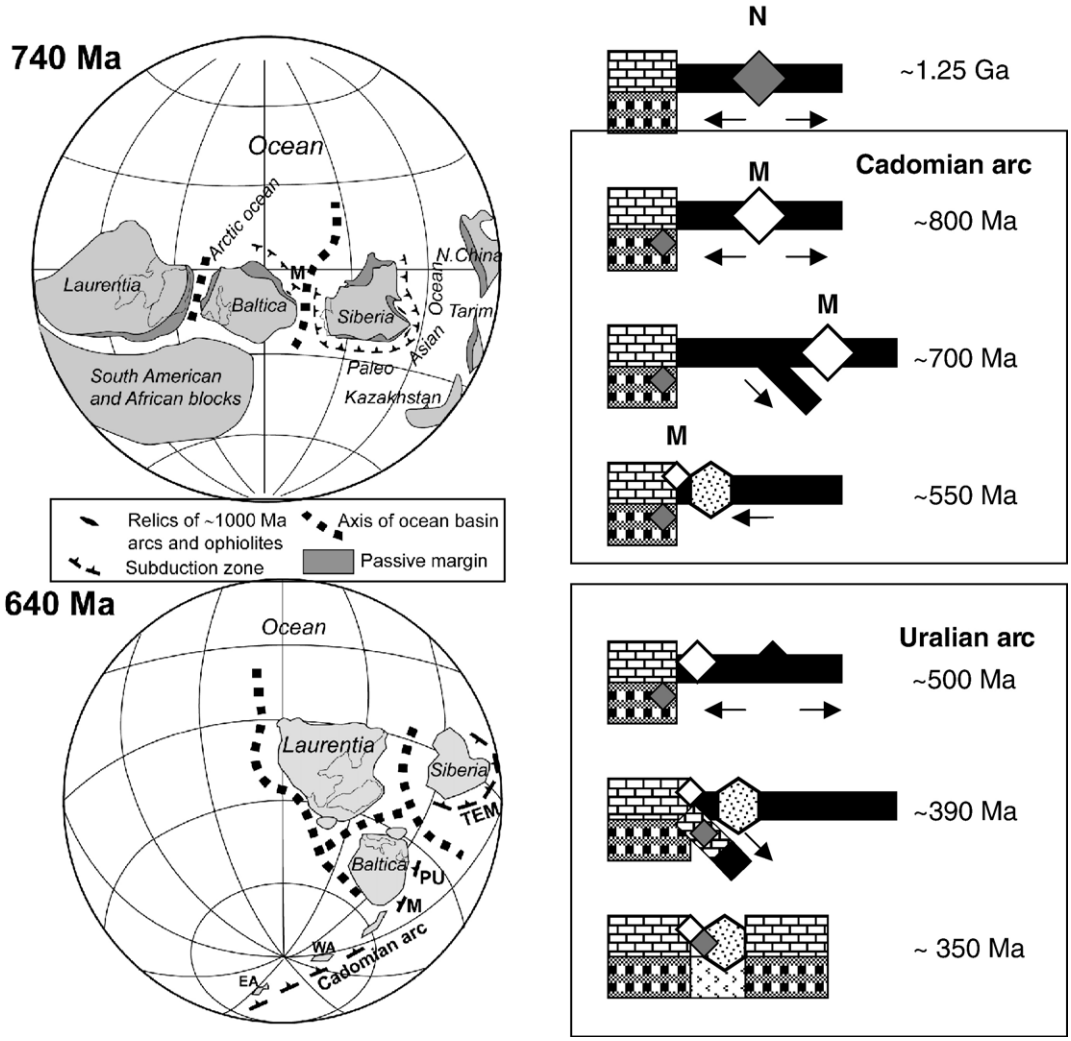

Fig. 14. (A) Reconstruction of continents bordering Baltica and the Paleo-Asian Ocean at ~ 740 and ~640 Ma (after Khain et al., 2003) during Cadomian island-arc development. M — Mindyak massif; PU — Polar Urals island-arc, including Enganepe ophiolite. All other continents have been omitted. (B) Schematic tectonic evolution of the Mindyak and Nurali massifs. M shows the Mindyak massif while N represents Nurali.

6.4.2. Neoproterozoic

Between ~ 850 and 650 Ma, the margins of the paleo-Asian ocean became the sites of new island-arc systems, which are today exposed in the Polar Urals in the Enganepe Range ophiolite (Scarrow et al., 2001). This ophiolite consists of a tholeiitic-arc–tholeiitic–adakite–OIB-like association, indicative of an intra-oceanic island-arc setting. A U–Pb zircon age (670± 5 Ma) from associated plagiogranites (Khain et al., 2003) shows that the ophiolitic rocks already existed in the late Neoproterozoic in the Polar Urals.

The Mindyak massif shows a complex tectonic evolution. The Sm–Nd age of the peridotites and the Re–Os age of upper gabbroic section indicate a Neoproterozoic (800–880 Ma) formation age for the peridotites and the overlying gabbros. The ε_{Nd} values for the peridotites ranging between 3.5 and 5, are lower than typical depleted mantle and could therefore be equivalent to the Enganepe ophiolite, which developed in an intra-oceanic island-arc setting. The Enganepe tholeiites as well as the gabbros from Mindyak massif are enriched in large-ion lithophile elements relative to MORB; this can be explained by subduction fluid addition (Scarrow et al., 1999, 2001).

The tectonic setting of the Mindyak massif between the Bashkirian anticlinorium to the west and Ilmenogorsk complex to the east may imply the existence of a paleo-ocean between these two crustal blocks during the

Late Proterozoic. If the Enganepe ophiolite is linked with the Cadomian arc, this arc must have continued along eastern Baltica all the way to the southern Urals (Fig. 14). In this case, the Mindyak ophiolite may be the first record of a Cadomian arc in the Southern Urals, as predicted by previous geodynamic reconstructions (Torsvik et al., 1996; Scarrow et al., 2001).

6.4.3. Paleozoic

The Mindyak massif has been affected by a later Paleozoic melt percolation, as shown by the coupled Re–Os and Sm–Nd isotope systematics, as well as by previous dating of metamorphosed gabbros (Scarrow et al., 1999). A minimum age of 467 Ma recorded in the cores of zircons found in these gabbros is close to the Re–Os age of 447±20 Ma for the mafic dykes (Fig. 8A), this can be considered as minimum age for the mafic volcanism. Around the same time, a rifting event affected the margin of the East-European (Baltica) craton, and led to the subsequent opening of the Uralian paleo-ocean. The Mindyak massif was probably incorporated in this rifting zone and thereafter intruded by gabbro dykes. The presence of garnet-bearing metagabbro within the Mindyak massif suggests that it has undergone high-pressure equilibration, which may be related to its exhumation along the continent–island-arc suture zone.

A later magmatic event has also affected the Nurali massif at ~ 400 Ma; this is consistent with published U–Pb data (Fershtater et al., 2000) and our Re–Os data (see Fig. 7C). The age might correspond to subduction of the Paleozoic oceanic crust and the formation of the Magnitogorsk island-arc (Puchkov, 1997). The ε_{Nd} ~ +5 (estimated at 390 Ma) for the gabbro and diorite samples from Nurali massif indicates a depleted mantle source. We can hypothesize that the Nurali peridotites were exhumed as a result of obduction and then intruded by Devonian mafic dykes. A similar model has been proposed for the formation of the high-P low-T Maksyutov complex within the Main Uralian Fault zone (Chemenda et al., 1997). The eclogite-facies mafic and felsic rocks of this complex and the related metamorphic event have been dated at 375±2 Ma by the Rb–Sr method (Glodny et al., 2002).

7. Conclusions

The major and trace element and Re–Os and Sm–Nd isotopic data presented in this study reveal the complex history for the Nurali and Mindyak lherzolite massifs in the southern Urals (see a summary in Table 5). Deciphering such a complexity is only possible by combining the whole-rock chemistry with these two isotopic systems.

The Re–Os data shows that the mantle sections of the peridotites were formed during the Proterozoic time. This confirms the predicted presence of Precambrian peridotites in Southern Urals proposed by Scarrow et al. (2001). Moreover, our data can help to reconstruct the Proterozoic history of the proto-Urals, which is still little known.

The Nurali peridotites are characterised by variable degrees of melt depletion, varying from low (5–10%) for the lherzolites up to moderate (up to 25%) for the dunites at the top of the Nurali mantle section. A multi-stage partial melting history for the Nurali peridotites is suggested by extremely low LREE contents and high Sm/Nd ratios. The Nurali transition zone cumulates show strong evidence for the isolation from the convecting upper mantle at ~ 1.25 Ga. At this stage, partial melting of mantle peridotites followed by fractional crystallisation produced layered cumulates in the Nurali massif, which were subsequently stored in the sub-continental lithosphere over 0.8 Ga. The age of the Nurali lherzolite-type ophiolite coincides with the age of the volcano-sedimentary Mashak formation within the adjacent Bashkirian mega-anticlinorium associated with the development of epicontinental rift basins on the passive margin of Baltica proto-continent. Rifting regimes associated with the break-up of the large Mesoproterozoic Eurasian continent into Baltica and Siberia existed at the same time on the passive margins of the Siberian and Kazakhstan–Tarim plates.

Most of the Mindyak peridotites were formed as residual material remaining after moderate degrees (>20%) of melting of already depleted parental peridotites. The younger Sm–Nd age obtained for the Mindyak peridotites (882±83 Ma) and the Re–Os age for associated gabbros (804±37 Ma) record a new tectonic event responsible for the separation of the Mindyak massif

Table 5
Summary of geochronological data obtained in this work using Re–Os and Sm–Nd isotope systematics, and possible geotectonic settings (see text for details)

Geotectonic event	Re–Os age, Ma	Sm–Nd age, Ma	Rock type
Continental rifting	1249±80		Wehrlites, Nurali
Rifting followed by subduction, Cadomian arc	804±37	882±83	Mindyak peridotites and gabbros
Rifting (Uralian ocean opening)	476±19	540±18	Mindyak gabbros
Subduction and Urals island-arc development	419±87	387±27	Nurali gabbro and diorites

from the convective mantle. Between ~850 and 650 Ma, the margins of the paleo-Asian ocean became sites of island-arc systems formation, as evident for example in Enganepe ophiolite in the Polar Urals. This ophiolite has then evolved in an intra-oceanic island-arc setting. Thus, the Mindyak lherzolite massif could be the first record of a Neoproterozoic Cadomian arc in Southern Urals.

The Urals development has reactivated existing ophiolite massifs, which were then dissected by mafic dykes. The Mindyak massif was involved in an Ordovician rifting zone around 440–470 Ma, which is compatible with the isochron ages obtained for the mafic dykes. During the Devonian, the Nurali massif was brought to the surface by subduction-related events, and was subsequently intruded by gabbro-diorite dykes.

It should be noted that the ages of mafic dykes are often used to date the associated ultramafic units. However, our coupled Re–Os and Sm–Nd study demonstrates that the mafic dykes are ~0.8 Ga (Nurali) and ~0.4 Ga (Mindyak) younger than the associated mantle units and are related to the later Palaeozoic Urals island-arc formation event. This suggests that the various units found in mafic–ultramafic sequences do not always have the same age and original tectonic setting. The depleted or slightly enriched mantle origin of the Nurali and Mindyak massifs has been demonstrated by combined Re–Os and Sm–Nd systematics. The range of ε_{Nd} values for the Mindyak peridotites (3.5 to 5) is lower than typical depleted mantle but is similar to that for the Enganepe ophiolite, which developed in an intra-oceanic island-arc setting. Nevertheless, the Nurali massif was most probably incorporated into the sub-continental lithospheric mantle in Proterozoic time. Thus, strictly speaking, it could be representative of young lithospheric mantle beneath the proto-Uralian mobile belt.

The complex history of the southern Urals peridotite massifs can be summarised in two stages: (1) the segregation of ultramafic bodies from a convecting asthenosphere followed by (2) the heating and percolation of partial melts associated with rifting events during the Paleozoic.

Acknowledgements

We are grateful to Giorgio Garuti, Federica Zaccarini and Eugeny Pushkarev for providing the samples of Mindyak and Nurali massifs. We thank Marc Davies for correction of English. This work was carried out in the framework of the EU-funded MinUrals project INCO COPERNICUS ICA2 CT-2000-10011. We thank Laurie Reisberg and the Editor S. L. Goldstein for their helpful reviews.

Appendix A. Supplementary data

Supplementary data associated with this article can be found, in the online version, at doi:10.1016/j.chemgeo.2007.02.006.

References

Barnes, S.J., Boyd, R., Korneliusson, A., Nilsson, L.P., Often, M., Pedersen, R.B., Robins, B., 1988. The use of mantle normalisation and metal ratios in discriminating between the effects of partial melting, crystal fractionation and sulphide segregation on platinum-group elements, gold, nickel and copper: examples from Norway. In: Prichard, H.M., Potts, P.J., Bowles, J.F.W., Cribb, S.J. (Eds.), Geo-Platinum, vol. 87. Elsevier, London, pp. 113–143.

Becker, H., Shirey, S.B., Carlson, R.W., 2001. Effects of melt percolation on the Re–Os systematics of peridotites from a Paleozoic convergent plate margin. Earth Planet. Sci. Lett. 188, 107–121.

Birck, J.-L., Roy-Barman, M., Capmas, F., 1997. Re–Os isotopic measurements at femtomole level in natural samples. Geostand. Newsl. 20, 19–27.

Bodinier, J.-L., Menzies, M.A., Thirlwall, M.F., 1991. Continental to oceanic mantle transition-REE and Sr–Nd isotopic geochemistry of the Lanzo lherzolite massif. J. Petrol. 191–210 (Spec. Iss.).

Boudier, F., Nicolas, A., 1985. Harzburgite and lherzolite subtypes in ophiolitic and oceanic environments. Earth Planet. Sci. Lett. 76, 84–92.

Brown, D.L., Juhlin, C., Alvarez Marron, J., Perez Estaun, A., Oslianski, A., 1998. Crustal-scale structure and evolution of an arc-continent collision zone in the Southern Urals, Russia. Tectonics 17 (2), 158–171.

Brueckner, H.K., Elhaddad, M.A., Hamelin, B., Hemming, S., Kröner, A., Reisberg, L., Seyler, M., 1995. A Pan African origin and uplift for the gneisses and peridotites of Zabargad Island, Red Sea. J. Geophys. Res. 100, 22283–22297.

Büchl, A., Brügmann, G., Batanova, V., Münker, C., Hofmann, A.W., 2002. Melt percolation monitored by Os isotopes and HSE abundances: a case study from the mantle section of the Troodos ophiolite. Earth Planet. Sci. Lett. 204, 385–402.

Burnham, O.M., Rogers, N.W., Pearson, D.G., van Calsteren, P.W., Hawkesworth, C.J., 1998. The petrogenesis of the eastern Pyrenean peridotites: an integrated study of their whole-rock geochemistry and Re–Os isotope composition. Geochim. Cosmochim. Acta 62, 2293–2310.

Chemenda, A., Matte, P., Sokolov, V., 1997. A model of Palaeozoic obduction and exhumation of high-pressure/low-temperature rocks in the southern Urals. Tectonophysics 276 (1–4), 217–227.

Edwards, R., Wasserburg, G.J., 1985. The age and emplacement of obducted oceanic crust in the Urals from Sm–Nd and Rb–Sr systematics. Earth Planet. Sci. Lett. 72, 389–404.

Ellam, R.M., Carlson, R.W., Shirey, S.B., 1992. Evidence from Re–Os isotopes for plume-lithosphere mixing in Karoo flood basalt genesis. Nature 359, 718–721.

Fershtater, G.B., Kotov, A.B., Smirnov, S.V., Pushkarev, E.V., Sal'nikova, E.B., Kovack, V.P., Yakovleva, S.Z., Berezhnaya, N.G., 2000. U–Pb zircon age of diorite from the Nurali lherzolite–gabbro massif in the Southern Urals. Dokl., Earth Sci. Sect. 371, 365–368 (in Russian).

Frey, F.A., Suen, C.J., Stockman, H.W., 1985. The Ronda high temperature peridotite: geochemistry and petrogenesis. Geochim. Cosmochim. Acta 49, 2469–2491.

Garuti, G., Fershtater, G., Bea, F., Montero, P., Pushkarev, E.V., Zaccarini, F., 1997. Platinum-group elements as petrological indicators in mafic–ultramafic complexes of the central and southern Urals: preliminary results. Tectonophysics 276, 181–194.

Glasmacher, U.A., Bauer, W., Giese, U., Reynolds, P., Kober, B., Puchkov, V., Stroink, L., Alekseyev, A., Willner, A.P., 2001. The metamorphic complex of Beloretzk, SW Urals, Russia — a terrane with a polyphase Meso- to Neoproterozoic thermo-dynamic evolution. Precambrian Res. 110, 185–213.

Glodny, J., Bingen, B., Austrheim, H., Molina, J.F., Rusin, A., 2002. Precise eclogitization ages deduced from Rb/Sr mineral systematics: the Maksyutov complex, Southern Urals, Russia. Geochim. Cosmochim. Acta 66 (7), 1221–1235.

Hamelin, B., Allègre, C.J., 1988. Lead isotope studies of orogenic lherzolite massifs. Earth Planet. Sci. Lett. 91, 117–131.

Hattori, K., Hart, S.R., 1991. Osmium–isotope ratios of platinum-group minerals associated with ultramafic intrusions: Os-isotopic evolution of the oceanic mantle. Earth Planet. Sci. Lett. 107, 499–514.

Hirose, K., Kushiro, I., 1993. Partial melting of dry peridotites at high pressures: determination of compositions of melts segregated from peridotite using aggregates of diamonds. Earth Planet. Sci. Lett. 114, 477–489.

Ionov, D.A., Ashchepkov, I., Jagoutz, E., 2005. The provenance of fertile off-craton lithospheric mantle: Sr–Nd isotope and chemical composition of garnet and spinel peridotite xenoliths from Vitim, Siberia. Chem. Geol. 217, 41–75.

Jagoutz, E., Palme, H., Baddenhausen, H., Blum, K., Cendales, M., Dreibus, G., Spettel, B., Lorenz, V., Wänke, H., 1979. The abundances of major, minot and trace elements in the Earth's mantle as defined from primitive ultramafic nodules. Proc. 10th Lunar Planet. Sci. Conf. , pp. 2031–2050.

Kamaletdinov, M.A., Kazantseva, T.T., 1983. Alloctonous Urals ophiolites. Nauka (168 pp. (in Russian)).

Khain, E.V., Bibikova, E.V., Salnikova, E.B., Kröner, A., Gibsher, A.S., Didenko, A.N., Degtyarev, K.E., Fedorova, A.A., 2003. The Palaeo-Asian ocean in the Neoproterozoic and early Palaeozoic: new geochronologic data and palaeotectonic reconstructions. Precambrian Res. 122, 329–358.

Knipper, A.L., Perfiliev, A.S.,1979. Ophiolite belt of the Urals. In: International Atlas of Ophiolites, IGCP Project 39, GSA Special Pub., map scale 1/2500000, 9–11.

Koroteev, V.A., Ivanov, K.S., Echtler, H.P., Ronkin, Y.L., 1997. Evolution of the Urals: complete geodynamic cycle during 1.6–0.2 Ga. Terra Abstr. 9, 118.

Loubet, M., Allègre, C.-J., 1982. Trace elements in orogenic lherzolites reveal the complex history if the upper mantle. Nature 298, 809–814.

Luck, J.-M., Allègre, C.J., 1991. Osmium isotopes in ophiolites. Earth Planet. Sci. Lett. 107, 406–415.

McDonough, W.F., Frey, F.A., 1989. Rare-earth elements in upper mantle rocks. In: Lipin, B., McKay, G.R. (Eds.), Geochemistry and Mineralogy of Rare-Earth Elements, pp. 99–145.

McDonough, W.F., Sun, S.-S., 1995. The composition of the Earth. Chem. Geol. 120, 223–253.

Meisel, T., Biino, G.G., Nägler, T.F., 1996. Re–Os, Sm–Nd, and rare earth element evidence for Proterozoic oceanic and possible subcontinental lithosphere in tectonized ultramafic lenses from the Swiss Alps. Geochim. Cosmochim. Acta 60, 2583–2593.

Meisel, T., Walker, R.J., Irving, A.J., Lorand, J.-P., 2001. Osmium isotopic composition of mantle xenoliths: a global perspective. Geochim. Cosmochim. Acta 65, 1311–1323.

Meisel, T., Reisberg, L., Moser, J., Carignan, J., Melcher, F., Brügmann, G., 2003. Re–Os systematics of UB-N, a serpentinized peridotite reference material. Chem. Geol. 201, 161–179.

Melcher, F., Grum, W., Thalhammer, T.V., Thalhammer, O.A.R., 1999. The giant chromite deposits at Kempirsai, Urals: constraints from trace element (PGE, REE) and isotope data. Miner. Depos. 34, 250–272.

Niu, Y., 1997. Mantle melting and melt extraction processes beneath ocean ridges: evidence from abyssal peridotites. J. Petrol. 38, 1047–1074.

Pearson, D.G., Davies, G.R., Nixon, P.H., 1993. Geochemical constraints on the petrogenesis of diamond facies pyroxenites from the Beni Bousera peridotite massif, North Morocco. J. Petrol. 34, 1–48.

Pearson, D.G., Shirey, S.B., Carlson, R.W., Boyd, F.R., Pokhilenko, N.P., Shimizu, N., 1995. Re–Os, Sm–Nd, and Rb–Sr isotope evidence for thick Archean lithospheric mantle beneath the Siberian craton modified by multistage metasomatism. Geochim. Cosmochim. Acta 59, 959–977.

Pearson, D.G., Irvine, G.I., Ionov, D.A., Boyd, F.R., Dreibus, G.E., 2004. Re–Os isotope systematics and platinum group element fractionation during mantle melt extraction: a study of massif and xenolith peridotite suites. Chem. Geol. 208, 29–59.

Pertsev, A.N., Spadea, P., Savelieva, G.N., Gaggero, L., 1997. Nature of the transition zone in the Nurali ophiolite, southern Urals. Tectonophysics 276, 163–180.

Puchkov, V.N., 1997. Structure and geodynamics of the Uralian orogen. In: Burg, J.-P., Ford, M. (Eds.), Orogeny through time. Geological Society, London, Special Publications, vol. 121, pp. 201–236.

Pushkarev, E.V., Kaleganov, B.A., 1993. K–Ar dating of magmatic complexes from the Khabarny mafic–ultramafic massif (South Urals). Rep. Acad. Sci., Ekaterinburg 328, 241–245 (in Russian).

Reisberg, L., Lorand, J.-P., 1995. Longevity of sub-continental mantle lithosphere from osmium isotope systematics in orogenic peridotite massifs. Nature 376, 159–162.

Reisberg, L.C., Allègre, C.J., Luck, J.-M., 1991. The Re–Os systematics of the Ronda ultramafic complex of southern Spain. Earth Planet. Sci. Lett. 105, 196–213.

Roy-Barman, M., Luck, J.-M., Allègre, C.J., 1996. Os isotopes in orogenic lherzolite massifs and mantle heterogeneities. Chem. Geol. 130, 55–64.

Savelieva, G.N., Sharaskin, A.Ya., Saveliev, A.A., Spadea, P., Gaggero, L., 1997. Ophiolites of the southern Uralides adjacent to the East European continental margin. Tectonophysics 276, 117–137.

Savelieva, G.N., Sharaskin, A.Ya., Saveliev, A.A., Spadea, P., Pertsev, A.N., Babarina, I.I., 2002. Ophiolites and zoned mafic–ultramafic massifs of the Urals: a comparative analysis and some tectonic implications. Geophys. Monogr. 132, 135–153.

Scarrow, J.H., Savelieva, G.N., Glodny, J., Montero, P., Pertsev, A., Cortesogno, L., Gaggero, L., 1999. The Mindyak Palaeozoic lherzolite ophiolite, Southern Urals: geochemistry and geochronology. Ofioliti 24 (2), 239–246.

Scarrow, J.H., Pease, V., Fleutelot, C., Dushin, V., 2001. The late Neoproterozoic Enganepe ophiolite, Polar Urals, Russia: an extension of the Cadomian arc? Precambrian Res. 110 (1–4), 255–275.

Sharma, M., Wasserburg, G.J., 1996. The neodymium isotopic compositions and rare earth patterns in highly depleted ultramafic rocks. Geochim. Cosmochim. Acta 60 (22), 4537–4550.

Shirey, S.B., Walker, R.J., 1995. Carius tube digestion for low-blank rhenium–osmium analysis. Anal. Chem. 34, 2136–2141.

Shirey, S.B., Walker, R.J., 1998. The Re–Os isotope system in cosmochemistry and high-temperature geochemistry. Annu. Rev. Earth Planet. Sci. 26, 423–500.

Torsvik, T.H., Smethurst, M.A., Meert, J.G., Van der Voo, R., McKerrow, W.S., Brasier, M.D., Sturt, B.A., Walderhaug, H.J., 1996. Continental break-up and collision in the Neoproterozoic and Palaeozoic — a tale of Baltica and Laurentia. Earth-Sci. Rev. 40 (3–4), 229–258.

Walker, R.J., Prichrd, H.M., Ishiwatari, A., Pimentel, M., 2002. The osmium isotopic composition of convecting upper mantle deducted from ophiolite chromites. Geochim. Cosmochim. Acta 66 (2), 329–345.

Walter, M.J., 2003. Melt extraction and compositional variability in the mantle. In: Holland, H.D., Turekian, K.K. (Eds.), Treatise on Geochemistry, vol. 2. Elsevier, Amsterdam, pp. 363–394.

Workman, R.K., Hart, S.R., 2005. Major and trace element composition of the depleted MORB mantle (DMM). Earth Planet. Sci. Lett. 231, 53–72.

Wu, F.Y., Walker, R.J., Ren, X.W., Sun, D.Y., Zhou, X.H., 2003. Osmium isotopic constraints on the age of lithospheric mantlebeneah northeastern China. Chem. Geol. 196, 107–129.

Zaccarini, F., Pushkarev, E.V., Fershtater, G.B., Cabella, R., Garuti, G., 2002. Platinum-group element mineralogy and geochemistry in chromites of the Nurali mafic–ultramafic complex (Southern Urals, Russia). 9th International Platinum Symposium Extended Abstracts, Billings, Montana, USA, pp. 487–490.